Adv Biochem Eng Biotechnol (2014) 138: 1–44
DOI: 10.1007/10_2013_187

Published Online: 23 April 2013

Dynamic Single-Use Bioreactors Used in Modern Liter- and m^3- Scale Biotechnological Processes: Engineering Characteristics and Scaling Up

Christian Löffelholz, Stephan C. Kaiser, Matthias Kraume, Regine Eibl and Dieter Eibl

Abstract During the past 10 years, single-use bioreactors have been well accepted in modern biopharmaceutical production processes targeting high-value products. Up to now, such processes have mainly been small- or medium-scale mammalian cell culture-based seed inoculum, vaccine or antibody productions. However, recently first attempts have been made to modify existing single-use bioreactors for the cultivation of plant cells and tissue cultures, and microorganisms. This has even led to the development of new single-use bioreactor types. Moreover, due to safety issues it has become clear that single-use bioreactors are the "must have" for expanding human stem cells delivering cell therapeutics, the biopharmaceuticals of the next generation. So it comes as no surprise that numerous different dynamic single-use bioreactor types, which are suitable for a wide range of applications, already dominate the market today. Bioreactor working principles, main applications, and bioengineering data are presented in this review, based on a current overview of greater than milliliter-scale, commercially available, dynamic single-use bioreactors. The focus is on stirred versions, which are omnipresent in R&D and manufacturing, and in particular Sartorius Stedim's BIOSTAT family. Finally, we examine development trends for single-use bioreactors, after discussing proven approaches for fast scaling-up processes.

Keywords Computational fluid dynamics · Engineering characteristics · Main applications · Scale-up · Single-use bioreactor types

C. Löffelholz (✉) · S. C. Kaiser · R. Eibl · D. Eibl
School of Life Sciences and Facility Management, Institute of Biotechnology, Zurich University of Applied Sciences (ZHAW), 8820 Wädenswil, Switzerland
e-mail: christian.loeffelholz@zhaw.ch

M. Kraume
Department Chemical and Process Engineering, Technische Universität Berlin, Straße des 17. Juni 135, 10623 Berlin, Germany

Abbreviations

1-D	1-dimensional
2-D	2-dimensional
3-D	3-dimensional
$A_{o,G}$	Interfacial area of gas bubbles
a	Specific interfacial area
B	Width of the bag
Bo	Bond number
c_m	Dimensionless mixing number
c_{o2}	Actual concentration of the oxygen in the liquid
c^*_{o2}	Saturation concentration of the oxygen in the liquid
c_s	Distance between stirrers
c_s/d_s	Ratio of stirrer distance to stirrer diameter
cv	Culture volume
C	Correlation factor
CFD	Computational fluid dynamics
CHO	Chinese hamster ovary cells
d_0	Shaking diameter
d_{32}	Sauter diameter
d_B	Bubble diameter
$d_{m,SF}$	Maximal shake flask diameter
d_s	Stirrer diameter
d_s/D	Ratio of the stirrer and bioreactor diameter
d_{SF}	Diameter shake flask
d_x	Cell diameter
D	Vessel diameter
D_I	Inner diameter of the container
DO	Dissolved oxygen
Do_2	Diffusion coefficient of oxygen
FDA	Food and Drug Administration
Fr	Froude number
FVM	Finite volume method
hMSC	Human mesenchymal stem cells
h	Stirrer height
h/D	Ratio of stirrer height and bioreactor diameter
h/H	Ratio of stirrer and liquid height
H	Height of the liquid
Ha	Hatta number
HCD	High cell density
H/D	Ratio of liquid height and bioreactor diameter
HTS	High-throughput screening
k	Rocking rate
k_H	Henry coefficient
k_L	Mass transfer coefficient

k_aL	Volumetric mass transfer coefficient
k_n	Reaction coefficient
L	Length of the bag
LBM	Lattice–Boltzmann method
LDA	Laser–Doppler anemometry
m	Slope in (26)
M	Torque
M_d	Dead weight torque (measured without liquid, representing only the bearing torque)
n	Reaction order
Ne	Newton number
N_S	Rotation frequency
OD	Optical density
OTR	Oxygen transfer rate
OUR	Oxygen uptake rate
P	Power input
P/V	Specific power input
PIV	Particle image velocimetry
PMP	Plant-made protein
p_{O2}	Oxygen partial pressure
PTV	Particle tracking velocimetry
q_{02}	Specific oxygen uptake rate
Re	Reynolds number
$\mathrm{Re}_{\mathrm{crit}}$	Critical Reynolds number
RT	Rushton turbine
S.U.B.	Single-use bioreactor from ThermoFisher scientific
SBI	Segment blade impeller
Sc	Schmidt number
t	Time
u_G	Superficial gas velocity
$u_{\max}$	Maximum velocity
u_{Tip}	Tip speed
V	Working volume
WIM	Wave-induced motion
X	Living cell density
x	Radial coordinate
x_1 and x_2	Empirical constants
XD	Extreme density
α	Volume fraction
β	Coefficient
γ_{NT}	Local shear gradients
$\gamma_{\mathrm{NT,\ m}}$	Mean local shear gradients
ε_{T}	Local energy dissipation rate
η	Viscosity

θ_m	Mixing time
λ	Kolmogorov length scale
ρ	Density

Contents

1 Introduction

The term "single-use" bioreactor (or "disposable" bioreactor) refers to the fact that the cultivation container is made of FDA-approved plastics (e.g., polyethylen, ethylenevinylacetate, polycarbonate, polystyrene) [1], and is only used once [2]. The cultivation container is typically provided in a sterile state and already pre-assembled, so that it can be used directly without further preparation. After finishing the bioprocess it is decontaminated and discarded. The resulting absence of sterilization and cleaning procedures allows products to be changed and new production campaigns to be started very quickly [3]. This finally leads to higher process flexibility, savings in time and costs, improvements in biosafety, and reduced environmental impact and waste, as has already been demonstrated in different studies with single-use bioreactors [4–6]. Sensor techniques [2], leachables/extractables (which can be secreted from plastic material and decrease product quality) [7], stability of the plastic material, and vendor dependence are among the main drawbacks of single-use bioreactors [8].

Nevertheless, advantages prevail, and single-use bioreactors have reached annual growth rates of 11 % [8] during recent years. This continuous growth can be ascribed to the international demand for rapid development, increased

manufacturing of new biotherapeutics (such as antibodies, hormones, enzymes, and vaccines), and an up to tenfold increase in the quantities of product titers that can be reached in these types of bioreactors [9, 10]. This last achievement explains the reduction of bioreactor size from 20 and 10 m^3 to 2 and 1 m^3 respectively, and the availability of single-use bioreactors in these smaller sizes.

Whereas single-use cultivation containers up to 50-L culture volume are rigid plastic vessels, cultivation containers for larger culture volumes are flexible, multi-layered plastic bags. These bags differ in their shapes and are 2-D pillowlike, 3-D cylindrical, 3-D cubes, 3-D with asymmetrical geometry or 3-D U-shaped. It is worth mentioning that trouble-free use of a flexible bag always requires a support container (dike or vessel often made from stainless steel) which supports the bag and keeps it in shape.

With the exception of single-use bioreactors developed for high-throughput screening (HTS), such as the Advanced MicroBioReactor System from TAP Biosystems [11, 12] or the Biolector from m2p-labs [13], and hollow fiber-based stem cell bioreactors such as the Quantum Cell Expansion System from CaridianBCT [14, 15], single-use bioreactors for milliliter-scale applications are normally not instrumented. These types of single-use bioreactors are not included in this chapter. In contrast, liter- and cubic meter-scale single-use bioreactors are equipped with standard or single-use sensors (installed either in situ or ex situ) to measure and control main process parameters such as pH and DO [16, 17]. However, single-use bioreactors are characterized by a lower level of instrumentation in comparison to reusable versions. In single-use bioreactors standard sensors are only regarded as a compromise inasmuch as their application requires the availability of 12-mm ports and aseptic connectors, or other special solutions. In addition, standard sensors need to be calibrated and sterilized before use, increasing the contamination risk. For this reason, single-use noninvasive and optical sensors are preferred by the majority of users.

2 Single-Use Bioreactor Types

The way for single-use bioreactors was paved by Fenwal‘s invention of the plastic blood bag in 1953 [18]. The first hollow fiber reactor was developed by Knazek et al. [19] in the early 1970s, followed by the replacement of CellFactories [20] and roller flasks. However, the development of further single-use bioreactors finally led to wave-mixed bioreactors [21, 22], which have increasingly displaced spinner flasks in seed inoculum productions since the early 2000s. Today the user can choose among a multitude of single-use bioreactors provided by different vendors. A systematization of single-use bioreactors that is analogous to that of their reusable counterparts was recommended by Eibl et al. [23, 24] and is based on the type of power input. Due to improved energy and mass transfer, dynamic single-use bioreactors have gained importance as scale has increased.

2.1 Current Overview

It can be clearly seen from Table 1, which summarizes commercially available liter- and cubic meter-scale dynamic single-use bioreactors, that mechanically driven wave-mixed and stirred systems represent the largest groups among the listed types. This development can be explained by the long-term experience of using stirred reusable bioreactors and the available knowledge in this area. The Wave was the first scalable single-use system that became accepted, despite its new mixing principle, wave-induced motion (WIM).

The WIM is caused by rocking or raising the platform containing the differently shaped single-use bags and is dependent on the bioreactor type (e.g. BIOSTAT CultiBag RM or AppliFlex). To date, six single-use bioreactor configurations from different vendors (the Wave Bioreactor, the BIOSTAT CultiBag RM, the Smart-Bag, the AppliFlex, the CELL-tainer and the XRS Bioreactor System) are in use for a wide range of production organisms including microorganisms [25], algae [26], plant cells [27], animal cells [28–30], bioactive T-cells [31, 32] and human mesenchymal stem cells (hMSCs) [33, 34]. As described by Ref. [27], power input and mass transfer are mainly influenced by the rocking rate, rocking angle, culture volume, culture broth viscosity and aeration rate. Along with WIM, bubble-free surface aeration in wave-mixed bioreactors results in more homogeneous energy dissipation and reduced foaming and flotation compared to stirred cell culture bioreactors. This is particularly the case for 1-D moving bags, which (in contrast to 2-D or 3-D moving bags) can exhibit limited power input and oxygen transfer for non-Newtonian fluids (e.g., plant cell suspensions) and aerobic microbial high cell density (HCD) cultivations. However, this problem is of less significance in animal cell-derived productions, where Newtonian fluid flow behavior is assumed. Scaling up of geometrically dissimilar wave-mixed single-use bioreactors (see also Sect. 5) is more problematic (maximum scale is limited; less knowledge of scale-up criteria exists), despite the fact that the sales literature highlights easy scalability as one advantage of this type of bioreactor.

As with wave-mixed bioreactors, mechanically driven, rotatory oscillating (BayShake Bioreactor [35]) and orbitally shaken single-use bioreactors (Current Bioreactor, OrbShake Bioreactor) contain no moving parts in the bag. They are surface-aerated and characterized by homogeneous energy dissipation and negligible foaming or flotation. Because they only recently entered cell culture labs, there are fewer application data available, even though bioengineering data have been determined and scale-up criteria proposed [4, 34, 36–38].

In Meissner‘s mechanically driven, oscillating, single-use Saltus Bioreactor (formerly VibroMix), the power input is adjustable through regulation of the motor amplitude and frequency [39]. An axial flow that mixes and aerates the cells in a cylindrical bag is caused by the movement of one or more perforated disks, which are fixed to an oscillating hollow shaft. The Saltus Bioreactor can generate high local power inputs and is designed for applications that are suited to medium to high shear conditions and culture broths with high viscosity. This means that this

Table 1 Current overview of commercially available liter- and cubic meter-scale single-use bioreactors

Working principle	Bioreactor brand	Max. cv	Vendor	References
Mechanically driven, oscillating movement, wave-mixed				
1-D WIM by rocking a pillowlike 2-D culture bag	Wave Bioreactor	500 L	GE Healthcare	[22, 44–49]
	BIOSTAT CultiBag RM	300 L	Sartorius Stedim Biotech	[25–28, 50–58]
	SmartBag	25 L	Finesse	[59]
1-D WIM by rocking a 3-D culture bag	AppliFlex	25 L	Applikon Biotech	[54, 60, 61]
2-D WIM by rocking a 3-D culture bag	CELL-tainer	125 L	Cellution Biotech	[56, 62– 64]
3-D WIM by rocking a 3-D culture bag	XRS Bioreactor System	25 L	Pall Life Sciences	[65]
Mechanically driven, rotatory oscillating				
3-D culture bag (cube-shaped)	BayShake Bioreactor	1 m^3	Bayer Technology Services	[4, 35, 66]
Mechanically driven, oscillation motion				
3-D culture bag with one or more vibrating disks	Saltus Bioreactor (in the past VibroMix)	100 L	Meissner Filtration Productions, Incorporation	[24, 39]
Mechanically driven, orbitally shaken				
3-D culture bag	CURRENT Bioreactor	300 L	AmProtein	[67–69]
	OrbShake Bioreactor	250 L	Satorius Stedim Biotech/Kühner	[36, 70–73]
Mechanically driven, stirred				
Rotating stirrer, magnetically coupled, 3-D culture bag	XDR	2 m^3	Xcellerex (now part of GE Healthcare)	[74–78]
	Mobius CellReady	200 L	Merck Millipore	[79–81]
	BIOSTAT CultiBag STR	1 m^3	Sartorius Stedim Biotech	[57, 82–86]
Rotating stirrer, mechanically coupled, rigid cylindrical vessel	UniVessel SU	2 L	Sartorius Stedim Biotech	[87, 88]
	Mobius CellReady	2.4 L	Merck Millipore	[21, 34, 89, 90]
	CelliGEN BLU Single-Use Bioreactor	50 L	Eppendorf	[91]
Rotating stirrer, mechanically coupled, 3-D culture bag	Single-Use Bioreactor (S.U.B.)	2 m^3	Thermo Fisher Scientific	[54, 64, 92–94]

(continued)

Table 1 (continued)

Working principle	Bioreactor brand	Max. cv	Vendor	References
Tumbling stirrer, magnetically coupled, 3-D culture bag (cube-shaped)	Nucleo Bioreactor	1 m^3	ATMI	[93, 95, 96]
Pneumatically driven				
Air Wheel design, 3-D culture bag (U-shape)	PBS Bioreactor	2 m^3	PBS Biotech	[40, 97]
Bubble column type, 3-D culture bag (asymmetrical geometry)	CellMaker Regular	8 L	Cellexus	[41–43]
Pneumatically driven and mechanically driven (hybrid)				
Combination of bubble column and stirred type, 3-D culture bag (asymmetrical geometry)	CellMaker Plus	50 L	Cellexus	[41]
Hydraulically driven				
Fixed bed type, 3-D culture bag	iCELLis	55 L $\approx$ 666 m^2	ATMI	[98–101]

Remark If not specially specified, the bag is cylindrical
cv culture volume

single-use bioreactor is not recommended for animal cell cultivations and processes with shear-sensitive plant cells.

Aeration and mixing in stirred single-use bioreactors, for which animal and microbial versions exist, is ensured by the aeration device (which is in most cases static) and rotating or tumbling stirrer(s) installed in the bag. A stirrer must be aseptically sealed, if it is not magnetically coupled, as is the case in the Mobius CellReady 3 L from Merck Millipore and the S.U.B. versions from ThermoFisher Scientific. Nevertheless, scaling-up of stirred single-use bioreactors is easier due to the geometrical similarity within a bioreactor family, which is normally based on reusable stirred cell culture bioreactors (compare also Sects. 3 and 4).

Pneumatically driven single-use bioreactors (Table 1) are applied for animal [40] and microbial [41–43] cultivations. They operate on the bubble column principle and provide homogeneous energy dissipation and high-efficiency mass transfer.

Disadvantages of bubble column bioreactors principally include bubble coalescence, strong foaming, and flotation. The currently available single-use, pneumatically driven bioreactors differ mainly in bag scale, shape and method of bubble generation. More detailed information about their working principles and characteristics are provided by Refs. [24 and 39].

Bubble column and stirring principles are combined in Cellexus's CellMaker Plus, a hybrid, single-use bioreactor, suitable for microorganisms, algae, and animal cells [41, 102]. The first hydraulically driven bioreactor with a bag is the ATMI's iCELLis, a single-use fixed bed bioreactor. The iCELLis uses medical-grade polyester microfiber macrocarriers, which provide capacity for HCDs, leading to high product titers in mammalian cell-based vaccine productions [98, 99]. As described by Prieels and Hambor [100, 101], this single-use bioreactor also allows successful expansion of hMSCs, where the scale is defined by the height of the bed.

2.2 Scale-Dependent, Potential Fields of Application

If focusing on potential fields of application for the previously described dynamic, single-use bioreactors, seven scale- and production-organism-dependent fields become evident (see Fig. 1). Production organisms are either grown as free or immobilized (bound to a carrier) cells. In most cases the bioreactors produce animal cell-derived products used in prophylaxis, diagnosis and therapy on a medium volume scale. They are mainly operated in fed batch (feeding) mode or, if HCDs and high-level protein titers are required, in perfusion mode [103]. For example, DSM Biologic's XD process [104] is a perfusion process that guarantees cell densities of around 1×10^8 cells/mL and antibody titers of around 25 g/L.

In seed inoculum productions, the wave-mixed BIOSTAT CultiBag RM and Wave Bioreactor have become widely accepted, whereas stirred, single-use bioreactors up to 1 m^3 are the systems of choice if mammalian cell-derived

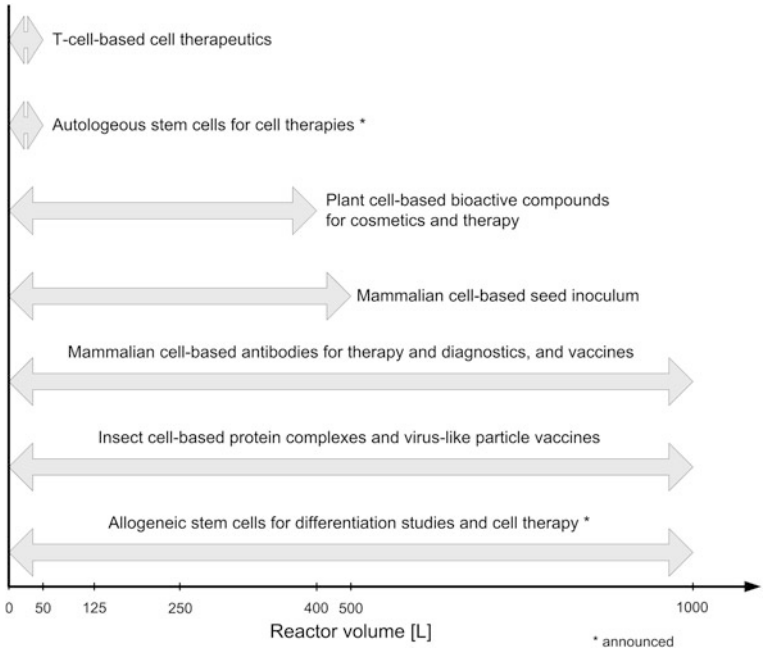

Fig. 1 Potential fields of application for dynamic single-use bioreactors exceeding mL-scale

therapeutics are the targeted products. Even though stirred single-use systems are already available up to 2 m^3, they have rarely been used. This is closely related to the more extensive operating procedures and training for staff, which both increase as culture volumes in single-use bioreactor bags rise.

If shear-sensitive cells (such as T-cells, bone marrow, or adipose tissue derived hMSCs) need to be grown, or if processes have to be realized, in which extensive foaming can occur (e.g., insect cell-based processes, where no chemically defined culture medium exists), wave-mixed single-use bioreactors should be chosen. As already mentioned in Sect. 2.1, they are characterized by homogeneous energy dissipation and low foam formation.

Wave-mixed bag bioreactors (up to a culture volume of 300 L) are also successfully used for the commercial production of plant-cell-derived secondary metabolites for cosmetics. Prominent product examples include the PhytoCELL-Tec products (*Malus domestica* Uttwiler Spätlauber, *Vitis vinifera* Gamay Teinturier Fréaux Grap, and *Arganium spinosum*) from Mibelle Biochemistry [105] and RESISTEM from Sederma [106]. As described by [26], existing photobioreactor versions are also suitable for microalgae cultivations. For the manufacturing of so-called plant-made proteins (PMPs) single-use bioreactors have rarely been used.

Nevertheless, there will be a demand in the future for single-use bioreactors for plant and microbial cell-derived high-value products that are not limited by mass transfer (energy and oxygen). Specially designed microbial versions of the CELL-

tainer and the XDR have proven themselves for HCD cultivations of *Escherichia coli, Pichia pastoris* and *Aspergilli* [63, 75]. ODs between 100 and 140 are also achievable for microorganisms grown in standard versions of the BIOSTAT CultiBag RM, as demonstrated by different groups [25, 82, 107]. In these cases there was either a low culture volume of 20 % or special feeding strategies were applied.

3 Bioengineering Characterization of Single-Use Bioreactors: Methods and Parameters

Knowledge of principal single-use bioreactor engineering parameters (such as mixing time, mass transfer coefficient, power input, fluid flow etc.) enables fast process optimization, scaling-up, and comparison of different types of bioreactors. The same methods were used to determine the bioengineering characteristics of the single-use bioreactors as for their reusable counterparts. Taking this into account, there is a differentiation between fundamental and advanced engineering methods. Methods that have been established and proven for single-use bioreactors and their resulting parameters are subsequently summarized and discussed.

3.1 Fundamental Engineering Characterization

In general, the flow regime in bioreactors can be characterized as laminar, transitional, or turbulent, depending on the dominance of viscous or inertial forces. This is characterized by the Reynolds number (Re), which is defined for stirred systems by (1) and depends on the stirrer diameter (d_S), speed (N_S) and liquid properties: liquid density (ρ_L) and viscosity (μ_L). It is well-known that the flow becomes fully turbulent above a critical Reynolds number that was found to be in the order of 1–10 $\times$ 10^4 for small- and medium-scale stirred bioreactors [88, 90, 108, 109], which is comparable to standard stirrer systems [59].

$$\mathrm{Re} = \frac{N_S \cdot d_S \cdot \rho_L}{\mu_L} \tag{1}$$

Similar relationships were introduced for orbitally shaken (e.g., shake flasks) [111] and rotatory oscillating bioreactors (i.e., the BAYSHAKE bioreactor) [35, 66], where Re is determined using the averaged rotational frequency and the maximum diameter of the mixing device. For shake flasks a critical Reynolds number of $\mathrm{Re} > 6 \times 10^4$ was found [112]. Wave-mixed systems with 2-D motion can be characterized by a modified Reynolds number given by (2), which is determined by the working volume (V), the width of the culture bag (B), the liquid level (H), the rocking rate (k) and an empirical constant that depends on the bag

type (*C*). This definition was derived from channel flows, providing a critical Re (Re_{crit}) of 1,000 [29].

$$Re_{mod} = \frac{V \cdot k \cdot C \cdot \rho_L}{\mu_L \cdot (2H + B)} \tag{2}$$

In addition to turbulence, the fluid flow in orbitally shaken bioreactors can be described by the "in-phase" and "out-of-phase" phenomenon, where the latter is characterized by liquid not moving in phase with the rotation of the shaker table [111]. A further parameter, which can often be easily related to the stirrer or vessel dimensions, is the maximum observable fluid velocity (u_{max}). Although, significantly higher tangential peak velocities were found in the stirrer wake region of Rushton turbines [113, 114] with regard to conventional stirrers, the maximum velocity in a number of different stirred single-use systems was found to correspond well to the stirrer tip speed (u_{Tip}) defined by (3) [90, 108, 109, 115].

$$u_{tip} = \pi \cdot d_S \cdot N_S \tag{3}$$

Furthermore, the tip speed of stirred systems is directly related to the impeller Reynolds number (4), which provides a first approximation of the maximum velocity at a desired turbulence. Because of shear sensitivity, a critical value of 1.0–2.0 m/s has been proposed [102].

$$Re \propto u_{Tip} \cdot d_S \tag{4}$$

In addition to these general criteria, the most important parameter for an engineering characterization is the volume-specific power input (*P*/*V*). Two approaches were developed for its determination: the torque method and the temperature method. The torque method, where the effective stirrer torque (difference in torque for stirring with liquid *M* and dead torque, M_d) is determined using a torque sensor (5), has become the standard method for conventional stirred vessels [116]. Consequently, this method was used for the measurement of the power input in the small-scale Mobius CellReady 3 L [90] as well as in the medium-scale BIOSTAT CultiBag STR 50 L [85, 86] and the S.U.B. Hyclone [108, 109]. The torque measurement was also shown to be feasible for shake flasks [117] and orbitally shaken cylindrical vessels [118, 119]. Therefore, the highest local energy input ε_{max}, which is often related to mechanical stress, is proportional to the specific power input under turbulent conditions (6).

$$P/V = \frac{(M - M_d) \cdot 2 * \pi \cdot N_S}{V_L} \tag{5}$$

$$P/V \propto \varepsilon_{max} \propto \frac{u_{Tip}^3}{d_S} \tag{6}$$

As an alternative, the temperature method was developed, where the power input is obtained from the heat balance given by (7), where $c_P \cdot w \cdot dT_F/dt$,

$U{\cdot}A{\cdot}(T_F{-}T_0)$ and $\mathrm{d}Q_0/\mathrm{d}t$ represent the change in temperature, the overall heat transfer rate through the vessel walls, and the heat-generating rate by the power consumption, respectively.

$$-c_p \cdot w \cdot \frac{\mathrm{d}T_F}{\mathrm{d}t} = U \cdot A \cdot (T_F - T_0) - \frac{\mathrm{d}Q_0}{\mathrm{d}t} \tag{7}$$

Although the torque method was expected to provide greater accuracy in terms of power consumption [118], because the power consumption can be obtained directly from the measured torque, results from both methods correlated reasonably well [119]. However, it should be emphasized that the power inputs investigated in these studies were in the range of 0.5 and 8 kW/m^3, which is much higher than typical values used for cell cultures in stirred systems, which are typically in the range of 0.01–0.25 kW/m^3 [120]. Thus, the temperature method may not be feasible for stirred or wave-mixed single-use systems, because of the much lower power input. Furthermore, when measuring the power consumption in small vessels, heat insulation is required, inasmuch as the temperature change from heat loss is relatively quick and leads to higher inaccuracies [118].

The power input of pneumatically driven bioreactors can be estimated from the superficial gas velocity (u_g) according to (8) if the isothermal expansion of gas is the predominant source of power [121]. However, no published data about specific power inputs for the pneumatically driven bioreactors were found.

$$\frac{P_G}{V_L} = \rho_L \cdot g \cdot u_G \tag{8}$$

Based on the power input, mixing and oxygen mass transfer can be estimated. Mixing (θ_m) is mostly characterized by the mixing time, defined as the duration required to achieve a defined degree of homogeneity after disturbance of the system (e.g., by change of temperature, concentration, conductivity, color, and/or density). In the majority of cases, 95 % homogeneity is accepted as adequate mixing performance. To determine mixing times two main approaches were applied: (de-)colorization methods and sensor methods.

Although the latter have the drawback of only measuring the mixing at specific locations, potentially leaving dead and rest zones hidden, these methods have been used to characterize different single-use bioreactors from benchtop to large-scale [80, 97, 122–125]. The advantages of the sensor methods are the precise data they deliver, reducing interobserver differences, and the fact that no optical accessibility is required, as is the case for (de-)colorization methods [116]. The main disadvantage of colorimetric methods is their inherent subjectivity, due to the personal view of the investigator. This may be overcome by automated image analysis, which has been used in mixing analysis of stirred single-use bioreactors [126].

For standard stirred bioreactors, it is well-known that the dimensionless mixing number (c_m), which represents the stirrer rotations required for the desired homogeneity (9), becomes constant under fully turbulent conditions [110]. It is not entirely surprising that the same relationship was confirmed for small- and

medium-scale single-use stirred vessels [90, 115]. Typical mixing numbers (c_m) for those systems are in the range of 20–40, leading to mixing times below 30 s for meaningful stirrer speeds in mammalian cell cultures.

$$c_m = N_S \cdot \theta_m \tag{9}$$

Based on turbulence theory, it was found that mixing time is inversely proportional to the third root of the specific power input under turbulent flow conditions. Furthermore, the mixing time is related to geometrical parameters leading to (10) which is valid for bioreactors where $H = D$ [120, 127].

$$\theta_m \propto \left(\frac{P}{V}\right)^{-1/3} \cdot \left(\frac{d_S}{D}\right)^{-1/3} \cdot D^{2/3} \tag{10}$$

For bioreactors with higher aspect ratios ($H/D > 1$), an additional term is introduced [i.e. $(H/D)^{2.43}$], which was originally developed for multiple impellers but has been shown also to take the influence of the filling height in single impeller systems into account [120]. This is represented by (11), which was shown to correlate well with mixing times in stirred single-use bioreactors predicted by CFD [115].

$$\theta_m \propto \left(\frac{P}{V}\right)^{-1/3} \cdot \left(\frac{d_S}{D}\right)^{-1/3} \cdot \left(\frac{H}{D}\right)^{2.43} \cdot D^{2/3} \tag{11}$$

Mixing in orbitally shaken bioreactors was found to be scalable by keeping the ratio of the inner diameter of the container (D_I) to the shaking diameter (d_{SF}) and the Froude number (Fr), defined by (12), constant [73]. Depending on the shaking speed, shaking amplitude, filling volume and vessel diameter, mixing numbers are between 5 and 80 for vessels of up to 1,500 L [73].

$$\mathrm{Fr} = \frac{2 \cdot \pi \cdot N \cdot (D_I + d_{SF})/2}{\sqrt{g \cdot D_I}} \tag{12}$$

In addition to mixing, oxygen mass transfer is considered to be the most important process during aerobic cultivation. The overall oxygen demand of the cells throughout the cultivation (OUR) must be met by the oxygen transfer rate (OTR). This demand is influenced by the specific oxygen uptake rate (q_{o2}) and increases as long as the number of viable cells (X) is also increasing, where c_{o2} and c^*_{o2} represent the actual and the saturated oxygen concentration respectively (13).

$$q_{o2} \cdot X = k_L \cdot a \cdot \left(c^*_{o2} - c_{o2}\right) \tag{13}$$

Oxygen transfer is mostly characterized by the overall volumetric mass transfer coefficient (k_La), which represents the product of the liquid mass transfer coefficient (k_L) and the specific interfacial area (a). For submerged aerated systems, the interfacial area depends on the local gas volume fraction (α) and the local bubble size represented by the Sauter mean diameter (d_{32}; 14).

$$a = \frac{A_{o,G}}{V_L} = \frac{6 \cdot \alpha}{(1-\alpha) \cdot d_{32}} \tag{14}$$

An approximate estimate of the gas–liquid interfacial area in surface-aerated, circular or cube-shaped vessels may be obtained from (15):

$$a = \frac{\pi \cdot D^2}{V_L} \text{ or } a = \frac{L \cdot B}{V_L} \tag{15}$$

However, it is notable that the bioreactor or surface motion will increase the interfacial area. For shake flasks, the interfacial area has been predicted to follow (16) for a fixed shaking diameter [128].

$$a \propto N^{0.6} \tag{16}$$

Although separate determination of the interfacial area in surface aerated systems was performed by image analysis [129], using an estimation of the evaporation rate [130], a chemical model system [131], and computational fluid dynamics (CFD) [128, 132], this remains difficult for submerged aeration because of the various factors affecting the local bubble size (aeration system, gas dispersion, media properties, etc.). Therefore, usually the k_La value is measured using either the gassing-out method or the sulphite method. Other methods, such as the respiratory gassing-out method, are of minor importance for engineering characterization in single-use bioreactors and are, therefore, not discussed in detail here (for more information please refer to Ref. [133]).

According to the definition, given in [116], in the gassing-out method the oxygen in the liquid is depleted by the introduction of nitrogen. After complete depletion, air is introduced leading to an increase in the oxygen concentration, where the rate of the concentration increase is determined by the k_La. Thus, the k_La can be obtained from the oxygen mass balance in the liquid (dc_{o2}/dt), which may be written for a totally mixed system by (17).

$$\frac{dc_{o2}}{dt} = k_La \cdot \left(c^*_{o2} - c_{o2}\right) \tag{17}$$

The gassing-out method is most often used in single-use systems above mL-scale independent of the type of power input (see Table 2). Typical k_La values achieved in stirred single-use bioreactors from benchtop to large scale are in the order of 5–40 1/h, depending on the scale, aeration rate and agitation. For example, k_La values of up to 35 1/h were achieved at typical cell culture agitation rates in the Mobius CellReady 3 L bioreactor with the microsparger [90, 134]. Similar values were found for the medium-scale BIOSTAT CultiBag STR 50 L at specific power inputs of 90 W/m^3 and an aeration rate of 0.1 vvm (see Sect. 4.5). In general, the k_La values in stirred bioreactors can be calculated by (18), where x_1, x_2 and C are bioreactor-dependent empirical constants. For the above-mentioned bioreactors, it was found that the influence of the superficial gas velocity was more pronounced than the specific power input P/V (i.e. $x_1 < x_2$). This is clearly

different from standard bioreactors used for microbial fermentations [135] and may be explained by the low gas dispersion capacities of the stirrers operated under typical cell culture conditions.

$$k_L a = C \cdot (P/V)^{x_1} \cdot u_G^{x_2} \tag{18}$$

Lower $k_L a$ values of between 4 and 20 1/h were reported in rocker-type wave-mixed systems with water and cell culture medium using typical process parameters for mammalian cells (6–10° rocking angle, 25–30 rpm, 0.25 vvm, 40–50 % filling level) [29]. In contrast, much higher $k_L a$ values of up to 700 1/h were reported for the CELLtainer, which is characterized by an additional horizontal displacement enabling much higher specific power inputs of up to 3.8 kW/m^3 [63]. As a result of such high oxygen transfer capacities, the cultivation of high oxygen demanding cultures may be realized without oxygen limitation.

However, it should be emphasised that results in surface-aerated systems obtained by the classical gassing-out method should be treated with caution because of the significant effect of the headspace gas composition. After introduction of nitrogen, the headspace is (nearly) free of oxygen, then increases continuously as the air supply is switched on again. During this process, the liquid saturation concentration changes with time according to Henry's Law ($p\mathrm{o}_2 = k_H * c^*_{\mathrm{o}2}$). Assuming a time-independent $c^*_{\mathrm{o}2}$, as given in (17), may lead to $k_L a$ being affected and to an erroneous effect of the aeration rate, which was confirmed by our own measurements [136] and is supported by data given in [137].

In the sulphite method, the depletion of oxygen is achieved by oxidation of sulphite ions to sulphate ions in the presence of a catalyst, such as copper, ferric, cobalt or manganese ions (19).

$$2\mathrm{SO}_3^{2-} + \mathrm{O}_2 \xrightarrow{\mathrm{Co}^{2+};\mathrm{Fe}^{-};\mathrm{Mn}^{+};\mathrm{Cu}^{+}} 2\mathrm{SO}_4^{2-} \tag{19}$$

Because the mass transfer phenomenon is coupled with a chemical reaction when using the dynamic sulphite method, the different sulphite oxidation regimes should be taken into account [138]. These can be classified by the Hatta number (Ha) defined by (20), where n, k_n and $D_{\mathrm{O}2}$ denote the reaction order for oxygen, the reaction constant, and the diffusion coefficient in the solution.

$$\mathrm{Ha} = \frac{\text{reaction rate}}{\text{mass transfer rate}} = \frac{\sqrt{\frac{2}{n+1} \cdot k_n \cdot \left(c^*_{\mathrm{o}2}\right)^{n-1} \cdot D_{\mathrm{O}2}}}{k_L} \tag{20}$$

Catalyst concentration, pH, temperature, and even light irradiation are the primary parameters that influence the reaction rate [139]. By using the film model, a reasonable approximation of the exact solution of the stationary mass balance can be derived for the absorption process (21) [140]. Measurements of the $k_L a$ have to be conducted in a nonaccelerated sulphite oxidation reaction regime, where Ha < 0.3 and the term α in (21; [131]) can be neglected [131].

Table 2 Overall oxygen mass transfer coefficients obtained by gassing-out method in different selected single-use bioreactor systems

System	Scale [L]	Agitation	Aeration rate [vvm]	k_oL [1/h]	References
Mechanically driven, stirred					
Mobius CellReady	3[a]	250 rpm	0.25	35	[90]
	200[a]	140 rpm	0.05	60	[80]
BIOSTAT UniVessel SU	3[a]	435 W/m^3	0.2	100	[146]
BIOSTAT CultiBag STR	50[b]	240 rpm	0.1	47	[85, 86]
	200[b]	240 rpm	0.1	37	[86]
Hyclone S.U.B.	50[b]	200 rpm	0.1	8.3	[125]
	200[b]	100 rpm	0.01	15	[23]
XDR-1000	1000[a]	132 rpm	0.015	9	[147]
Mechanically driven, oscillation motion					
BayShake Bioreactor	32[b]	120°, 210 W/m^3	n.a.	20	[35]
Pneumatically driven					
PBS bioreactor	n.a.			20	[148]
Mechanically driven, oscillating movement, wave-mixed					
AppliFlex Bioreactor	2.5[b]	6°, 24 rpm	0.5	14.6	[61]
	5[b]	11°, 25 rpm	0.5	24	[61]
	10[b]	4°, 20 rpm	0.025	4.4	[29]
Biostat CultiBag RM	1[b]	n.a.	n.a.	22	[57]
	10[b]	n.a.	n.a.	6	[57]
BioWave Bioreactor	1[b]	6°, 30 rpm	0.25	10	[29]
	10[b]	5°, 30 rpm	0.25	9.3	[29]
	100 L[b]	10°, 24 rpm	0.25	5.6	[29]
CELL-tainer	10[b]	20°[c]	n.a.	≈700	[63]
Mechanically driven, orbitally shaken					
OrbShake bioreactor SB200-X	100[b]	70 rpm	n.a.	27	[70]

[a] total volume, [b] working volume, [c] 20-cm displacement, n.a. not available

$$\mathrm{OTR} = \sqrt{\underbrace{\frac{2}{n+1} \cdot k_n \cdot \left(c^*_{o2}\right)^{n-1} \cdot D_{O2}}_{\alpha} + \underbrace{k_L^2}_{\beta}} \cdot a \cdot \left(c^*_{o2} - c_{o2}\right) \tag{21}$$

The sulphite method was primarily used in noninstrumented, small-scale systems, such as microtiter plates [131, 138], Tubespin reactors [141], shake flasks [142], and the BioLector [143]. Volumetric oxygen transfer coefficients of up to 200 1/h have been observed in 96-well microplates operated at high shaking frequencies (n_{SF}) of over 1000 rpm [130]. Correlating k_La by dimensionless groups, (22) was obtained, where Sc and Bo denote the Schmidt number $(\mu/(\rho \cdot D))$ and the Bond number $(\rho \cdot d^2 \cdot g/\sigma)$ respectively, and x and y are dependent on the microplate geometry.

$$k_L a = 31.35 \cdot D_{O2} \cdot a \cdot \mathrm{Re}^{0.68} \cdot \mathrm{Sc}^{0.36} \cdot \mathrm{Fr}^{x} \cdot \mathrm{Bo}^{y} \quad (22)$$

Lower values for $k_L a$ of up to 104 1/h were found for shake flasks with 200 mL working volumes at agitation rates of 210 rpm [141]. Comprehensive investigations of oxygen mass transfer have been carried out by Büchs and his co-workers, who found that the "out-of-phase" phenomenon (see above) has an adverse effect on the oxygen mass transfer [144]. The data could be correlated to the maximum oxygen transfer capacity (mmol/L/h) by (23), where the rotational speed n is given in rpm, the shaking diameter d_0 and the flask diameter in cm and the working volume in mL [142].

$$\mathrm{OTR}_{\max} \propto n_{\mathrm{SF}}^{0.84} \cdot V_L^{-0.84} \cdot d_0^{0.27} \cdot d_{m,\mathrm{SF}}^{-1.25} \quad (23)$$

Further engineering characterization, such as determination of residence time [29, 145] and heat transfer [118], are of minor importance for single-use bioreactors and only few reports are available in the literature. This may be explained by the fact, that single-use bioreactors are primarily used for cell culture applications, where low feeding rates are used, leading to significantly longer residence times compared to mixing time, and almost no heating or cooling limitations. Nevertheless, heating and cooling may become problematic in a microbial process performed in single-use bioreactors.

3.2 Advanced Engineering Characterization

Advanced engineering methods are applied to gain local and instantaneous values for the fluid flow, which, in addition to the previously described criteria that are considered as volume-averaged parameters, can be used for bioreactor characterization and scaling-up. Keeping in mind that the fluid flow in bioreactors can be very heterogeneous, the "global" parameters may not be sufficient for an advanced characterization. For example, it is well-known that the stirrer power is only dissipated in a small fraction of the bioreactors and the maximum dissipation rate is 100–200 times higher than the volume-average [149]. This may have an intrinsic effect on shear-sensitive organisms.

Some attempts have been made to characterize local fluid flow in single-use bioreactors by measuring fluid velocities using particle image velocimetry (PIV) [108], particle tracking velocimetry (PTV) [150], laser Doppler anemometry (LDA) [109], and hot-film anemometry [151]. The latter method has the drawback of affecting the flow, because the probe must be positioned inside the liquid. Therefore, the contactless, laser-based PIV and PTV methods are preferred. However, although these experimental methods are reliable, they are too time consuming to characterize the complete 3-D fluid flow within a typical bioreactor [152]. Thus, numerical methods are used to overcome this limitation and, of these methods, CFD has become the most important approach in recent years.

The fundamentals of CFD are based on mass, momentum and energy conservation equations, which are second-order partial differential equations that, for the most part, cannot be solved analytically. Thus, different numerical methods, such as the finite volume method (FVM) or the Lattice–Boltzmann method (LBM) are used to render the flow field. In each case, the fluid domain is divided into a discrete number of elements and the conservation equations are solved for each volume element. Details of the numerical basics and the algorithms used are provided elsewhere [153–157].

CFD has been applied for characterization of fluid flows in different stirred [88, 90, 108, 109, 158] and wave-mixed bioreactors [29, 151], orbitally shaken flasks [128], microtiter plates [159], the rotatory oscillating BayShake Bioreactor [35], and the pneumatically driven PBS Bioreactor [109]. The main advantage of CFD is that local and time-resolved data about the fluid flow (e.g., pressure, turbulence, shear stress) as well as physical and chemical properties (e.g., concentrations, viscosity, density, gas hold-up) can be obtained.

The local specific energy dissipation rate (ε) is considered to be an important parameter that can be predicted using CFD. This can be used to calculate the Kolmogorov micro-scale of turbulence (λ) in turbulent flows defined by (24). The turbulence micro-scale defines the size of the smallest turbulent eddies. Various studies have proposed that cell damage occurs in bioreactors, if the size of these eddies is comparable to the biological entity (i.e. $\lambda/d_X \approx 1$) [160–162]. However, this theory is yet to be proven and there are some doubts inasmuch as it does not take the physical properties of the cells into account [120, 127].

$$\lambda = \left(\frac{\mu^3}{\rho_L^3 \cdot \varepsilon}\right)^{1/4} \tag{24}$$

Furthermore, ε is often used to predict oxygen mass transfer, based on Higbie's penetration theory [163, 164]. Here, the liquid oxygen mass transfer coefficient is related to the surface renewable rate resulting in (25).

$$k_L = \frac{2}{\sqrt{\pi}} \cdot \sqrt{D_{O2}} \cdot \left(\frac{\varepsilon \cdot \rho_L}{\mu_L}\right)^{1/4} \tag{25}$$

Together with the specific surface area a, the k_La, which has been shown to be spatially heterogeneous, not only in large-, but also in small-scale bioreactors, can be predicted using CFD [88, 90]. However, special two-phase models that are not discussed here in detail, which take momentum exchange of the continuous and dispersed phases into account, are required. Detailed information is provided in Ref. [156].

4 Bioengineering Data of the UniVessel SU and BIOSTAT CultiBag STR

The following case study presents a possible approach for the engineering characterization of small- to medium-scale, stirred, single-use bioreactors. For this purpose, the two single-use bioreactor systems UniVessel SU and BIOSTAT CultiBag STR from Sartorius Stedim Biotech were chosen because they are as close as possible to the design and instrumentation of conventional glass or stainless steel cell culture bioreactors. The rigid UniVessel SU (Fig. 2a) is equipped with two-stage segment blade impellers with a blade angle of 30°. The impellers have a diameter of 0.055 m and are mounted with an impeller distance (c_s) of 0.07 m. The diameter of the cylindrical vessel (D) increases towards the top (from 0.118 to 0.126 m), caused by the validated manufacturing process. The ratio of liquid height to vessel diameter (H/D) is 1.3 and ensures a maximum working volume of 2 L. The bioreactor can be equipped either with conventional probes or optical sensors and is unbaffled.

In the case of the BIOSTAT CultiBag STR product line, the cultivation vessel is a flexible 3-D bag, which has to be mounted in a stainless steel support housing (Fig. 2b). Two different top-driven stirrer configurations are available: a combination of a Rushton turbine (RT) and SBI or two SBIs. Irrespective of the configuration, the stirrer diameters are 0.37, 0.23, 0.31, and 0.38 m for the corresponding working volumes of 50, 200, 500, and 1,000 L, respectively. However, the BIOSTAT CultiBag STR line primarily differs from the smaller-scale series in the differently shaped bottoms of the cultivation vessels. The other geometric parameters (e.g. d_s/D, H/D, c_s/d_s etc.) are similar for all the different size bags in the unbaffled BIOSTAT CultiBag STR line (for details see Refs. [85, 86]) and, therefore, fulfill the scale-up criteria. The measurement of pH and dissolved oxygen are realized using small optical sensors, which have no significant influence on the fluid flow, and no additional elements are installed.

In order to characterize the UniVessel SU and the BIOSTAT CultiBag STR line using CFD, the ANSYS Fluent commercial software package was used.

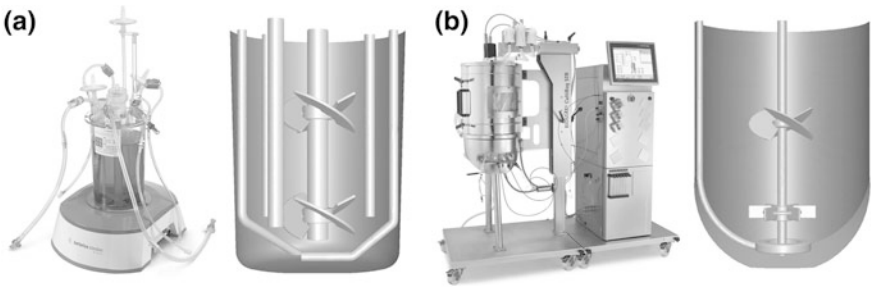

Fig. 2 The stirred single-use cell culture bioreactors from Sartorius Stedim with the UniVessel SU (**a**) and the BIOSTAT CultiBag STR with a working volume of 50 L (**b**)

Depending on the maximum working volume, the fluid domains of the nine different bioreactor configurations were divided into unstructured, body-fitted grids with up to approximately 5-mio volume elements. PIV was used for experimental measurement of the fluid flow in a 50 L vessel. In the systems with volumes of up to 200 L, the power input was determined using the torque method and the mixing time was predicted by the decolorization method.

4.1 Fluid Flow Pattern and Velocity Distribution

In Fig. 3, the ungassed fluid flow pattern obtained using CFD and PIV are compared for the mid-vessel plane (x–y-plane). The velocity components in the x- and y-directions are considered and the values are normalized by the tip speed (u_{Tip}). The highest fluid velocity magnitudes are found near the impeller tips and correspond well with the calculated tip speed (u_{Tip}) of 1.05 m/s using (3) (data not shown), which creates fully turbulent conditions (see Sect. 4.2).

In the BIOSTAT CultiBag STR 50 L with two SBIs (Fig. 3a, b), the highest relative velocity of 0.45 u_{Tip} occurs at the outer blade edges. Along the blade discharge the relative velocities decrease down to 0.3 u_{Tip} and a swirl in the axial direction can clearly be seen. This results in fluid recirculation along the vessel wall towards the fluid surface and the stirrer shaft. Here, the relative velocities range between 0.03 and 0.15 u_{Tip}. Due to prevailing axial swirls next to the impeller discharge of the two segment blade impellers, an axial fluid flow pattern and a similar velocity distribution can be observed for both the numerical and experimental methods. In summary, the CFD model can be considered as valid, because the numerically and experimentally obtained results visually agree [165–167]. Furthermore, the obtained fluid flow pattern corresponds well to patterns seen for conventional stirrers.

In the case of the RT + SBI stirrer configuration (Fig. 3c, d), the upper SBI clearly shows an axial flow profile in down-pumping mode with a maximum velocity of 0.45 u_{Tip}, whereas the lower RT discharges the fluid radially towards the vessel wall. The CFD simulation shows a maximum relative velocity of 0.51 u_{Tip} (x- and y-direction), which develops close to the impeller. In the predicted fluid flow pattern, the upward-forming loop represents the major flow, caused by the downward-inclining blade discharge. This results in a less pronounced swirl along the bottom wall. The experimental investigations reveal that the fluid is discharged radially, impinges on the outer wall, splits, and moves up and down, forming two recirculating loops in each vessel half. The interaction of the two impellers can be ignored if the c_s/d_s ratio exceeds 1.25 [110], which is true in the present case. In contrast, a slight downward tendency in the impeller discharge was observed in different experimental [168, 169] and numerical investigations [170] using RT in fully baffled and unbaffled vessels under turbulent conditions.

A more quantitative analysis is given in Fig. 3e, where radial profiles of the normalized fluid velocities for different heights in the BIOSTAT CultiBag STR

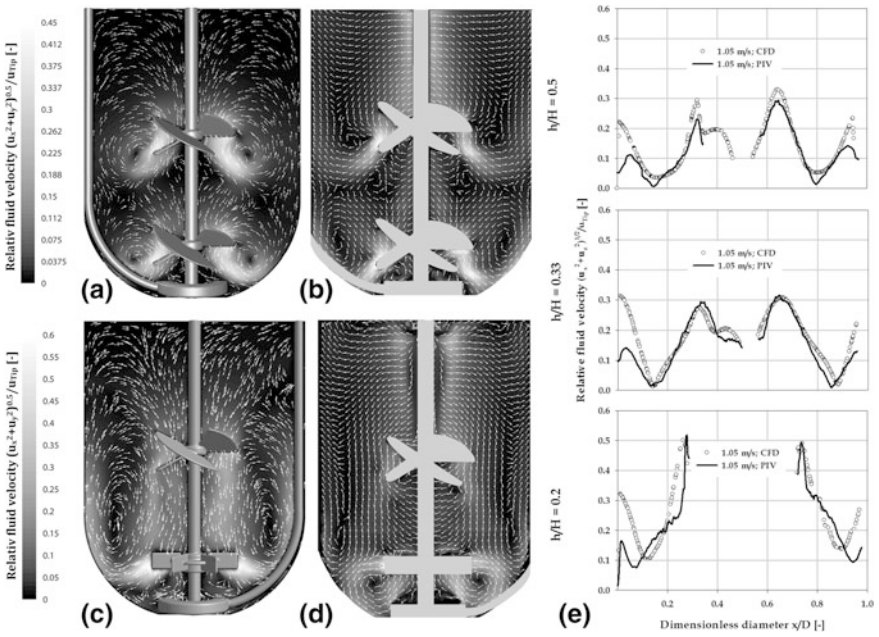

Fig. 3 Evaluation of the BIOSTAT CultiBag STR 50 L for both stirrer configurations. The numerical and experimental fluid flow patterns for the 2 × SBI configuration is shown in **a** and **b**, and for the RT + SBI configuration in **c** and **d**. A quantitative analysis of the relative velocity as a function of dimensionless diameter is provided in **e** for different dimensionless heights (mid-plane of RT and SBI as well as in the middle of both stirrers)

50 L with RT and SBI (Fig. 3e) are presented. Almost identical velocity distributions were found a third and half-way up the vessel height ($h/H = 0.33$; $h/H = 0.5$), with deviations towards the vessel walls. This may be explained by both numerical and experimental uncertainties resulting from optical distortions. The up to 60 % lower relative velocities were obtained in the experimental approach. However, the maximum and minimum velocities that were predicted for the impeller discharge and the point of flow reversal (where up- and downward flow meet) were well captured by PIV, with deviations below 10 %. For the rest of the velocity profile, the two different methods correlate sufficiently, with a maximum deviation of 10 %. However, the two graphs do not correlate if h/H is 0.5 or x/D is 0.35 (Fig. 3e). This inconsistency is based on the experimental measurement technique where the SBI covers the fluid and thus prevents determination. The above-mentioned deviating circulation flow is clearly shown in the velocity distribution profile of $h/H = 0.2$. Here, the maximum relative velocity of 0.51 u_{Tip} decreases similarly along the blade discharge towards the vessel wall ($0.1 < d_s/D < 0.3$ and $0.7 < x/D < 0.9$). Compared to the experimental investigation, the CFD simulation predicts a 0.05 x/D reduced discharge, causing a downward fluid flow (Fig. 3e). In addition, the velocities near the vessel wall differ by up to 45 %

when comparing the two methods. However, further experimental investigations of power input and mixing times are recommended in order to compare the methods and assess the influence of different fluid flows on biochemical engineering parameters.

4.2 Power Input

The power input represents the most important criterion for scaling-up of bioreactor systems [171]. Consequently, determining this was one of the major tasks of this case study to characterize and compare the UniVessel SU and the BIOSTAT CultiBag STR versions. By using CFD, the power input (P) in the BIOSTAT CultiBag STR 50 L was determined by the torque at the stirrer elements (1 and 5). It was demonstrated that, while exceeding a critical Reynolds number (Re_{crit}) of 10^4, a turbulent flow regime is reached when the Newton number (Ne) becomes a constant with values of 1.1 for the 2 × SBI configuration and 3.1 for the RT + SBI configuration [88]. Thus, the values obtained for Re_{crit} and Ne are comparable to those for conventional glass or stainless steel bioreactors [110, 172, 173]. Furthermore, the CFD predicted and experimentally determined power inputs were very similar [85, 86] with a maximum deviation below 15 %.

The tip speed was increased up to a maximum u_{Tip} of 1.8 m/s, which has been proposed as the maximum tolerable fluid velocity for mammalian cells [160]. At such high tip speeds, the maximum P/V of about 86 and 240 W/m^3 were obtained for the 2 × SBI configuration and the RT + SBI configuration, respectively (Fig. 4a). Henzler and Eibl and Eibl propose a maximum specific power input of 100 W/m^3 to avoid any cell damage [102, 174], although, a higher range of up to 250 W/m^3 is suggested by Nienow [120].

An additional analysis of the power input was carried out for aerated conditions. Although the effect of aeration is normally negligible, due to the low gassing rates used for mammalian cell cultures, the total power input (P/V) is usually applied to make a comparison or to scale up bioreactors [120, 175]. For the two stirrer configurations, the determined aerated P/V values obtained for an aeration rate of 0.02 vvm follow the same trend as the unaerated power input (see Fig. 4a), with a mean increase of 15 %. This could be verified by experimental data (not shown). The numerically and experimentally obtained results for the BIOSTAT CultiBag STR 50 L correlated well, therefore determination of P/V was also carried out for the UniVessel SU and the BIOSTAT CultiBag STR 200, 500 and 1000 L, for both stirrer configurations. In Fig. 4b the results are presented as a function of u_{Tip}. If u_{Tip} is used as a scale-up or scale-down criterion, P/V increases significantly for smaller volumes, but decreases for large volumes and is described by the relation in (6). Therefore, in the UniVessel SU the maximum P/V is about 435 W/m^3, which is unreasonably high for cell culture applications, but sufficient for microbial fermentations. Reasonable power inputs for cell culture applications of up to 150 W/m^3 have already been achieved with medium values of u_{Tip} in the range of

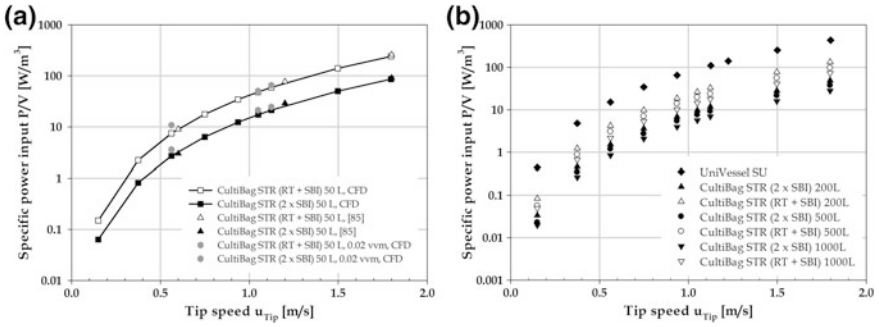

Fig. 4 Comparison of numerical and experimental investigations of the specific power input as a function of tip speed in the BIOSTAT CultiBag STR 50 L under unaerated and sparged conditions (**a**). Comparison of the CFD-predicted specific power input as a function of tip speed for all bioreactor sizes and configurations (**b**)

0.5–1.25 m/s. For these values, Re is between 0.8 and 2×10^4, indicating turbulent fluid flow, for a constant Newton number of 1.5.

In the case of the BIOSTAT CultiBag STR with working volumes of 200, 500, and 1,000 L (Fig. 4b), the *P/V* behaves according to (6). Considering the maximum *P/V* for the 50 L bioreactor with $\sim$86 W/m^3 ($2 \times$ SBI) and $\sim$240 W/m^3 (RT + SBI), the power inputs in the 200-L bioreactors are only $\sim$48 W/m^3 ($2 \times$ SBI) and 133 W/m^3 (RT + SBI). P/V decreases even further in the 1,000-L bioreactors so that $\sim$28 W/m^3 ($2 \times$ SBI) and $\sim$73 W/m^3 (RT + SBI) are achieved. The numerically determined Ne numbers of 1.1 and 2.8 ($2 \times$ SBI/RT + SBI) diverge only slightly from the values for the 50-L bioreactors, which can be explained by the minor differences of the dimensionless ratios of the reactor geometry for the various sizes.

In summary, it could be demonstrated that the numerically determined engineering parameters (Re_{crit}, Ne, *P/V* range) agree excellently with the experimentally obtained results. Furthermore, it could be shown that the characteristics of the investigated single-use bioreactors are comparable to those of conventional cell culture bioreactors.

4.3 Mixing Time

The characterization of the mixing behavior in the investigated single-use bioreactors was performed dependent on u_{Tip} using an identical range of up to 1.8 m/s (see Sect. 4.2). For this purpose, the concentration was determined, after addition of an inert tracer with identical fluid properties to the vessel contents. The tracer concentration was predicted transiently using a numerical method, however, the flow field of the steady simulation was "frozen". The CFD predicted mixing times were validated by comparing experimental data. The iodometrical decolorization

[116] (UniVessel SU) and conductivity methods [85] (BIOSTAT CultiBag STR) were applied, and 95 % mixing was assumed.

Figure 5a depicts the experimentally and numerically obtained mixing times (θ_m) for the UniVessel SU and the BIOSTAT CultiBag STR 50 and 200 L, which are presented as a function of P/V. Turbulence increases as power input rises, therefore this directly leads to a decrease in the mixing time [172]. Although about 100 s are required to achieve the desired 95 % homogeneity in the UniVessel SU at lowest power input (0.5 W/m^3), only about 3 s are required at the maximum power input (435 W/m^3). In the BIOSTAT CultiBag STR (2 x SBI), the numerical mixing times range between 10 and 60 s for the 50-L bioreactor (0.8–86 W/m^3), and between 20 and 60 s for the 200-L scale (1.5–49 W/m^3). Therefore, the mixing times of the BIOSTAT CultiBag STR are in the same range as for the UniVessel SU. Although it was found that fluctuations in the tracer concentrations were underpredicted by the applied RANS approach using the k-ε turbulence model, the mixing times correlate fairly well [176, 177]. Comparison of the numerically and experimentally determined mixing times (Fig. 5a) shows a maximum deviation below 4 % for the UniVessel SU. Higher deviations were found for the BIOSTAT CultiBag STR systems, where mixing times differ by up to 18 %, which can be ascribed to uncertainties in both experimental and CFD predicted data.

Based on similar results obtained for the UniVessel SU, the mixing times in the BIOSTAT CultiBag STR line with RT + SBI (Fig. 5b) and SBIs (data not shown) were analyzed. As shown in Fig. 5b, the mixing time decreases with increasing working volume and decreasing specific power input. This results in a mixing time ranging between 13 s (50 L; 240 W/m^3) and 200 s (1,000 L; 0.05 W/m^3) for the stirrer configuration of RT + SBI. However, in cell culture processes a power input in the range of 1 up to 150 W/m^3 is required and here the mixing times are between 15 and 75 s. The numerically determined mixing number (c_m) specifies the number of rotations required to achieve the desired homogeneity and is 29 ± 5. In addition, the exponent of −0.32 of the regression line (Fig. 5 B) is roughly equivalent to the theoretically cited exponent of −0.33, which is obtained under turbulent flow conditions [178]. In the BIOSTAT CultiBag STR (2 × SBI), the determined mixing times are on average 30 % higher considering the entire operation range. According to this, the homogenization number is 34 ± 1, whereas the exponent of the regression line is identical to the theoretical value (data not shown). In summary, the comparison of the results from the CFD simulation and the experimental measurements agree well ($c_H > 95$ %, 80 % $< \theta_m <$ 100 %).

4.4 Mechanical Stress

The spatially resolved data obtained by CFD can also be used to evaluate mechanical stress that can potentially damage cells. The turbulence, the formation of eddies [179, 180], and velocity gradients [160, 181] are considered potential

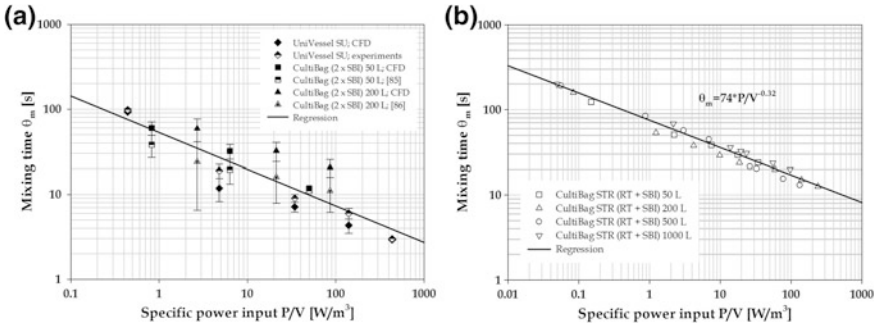

Fig. 5 Comparison of numerical and experimental mixing times as a function of specific power input in the UniVessel SU and the BIOSTAT CultiBag STR 50 L and 200 L (**a**). The error bars indicate the simple standard deviation of the mixing times. Additionally, the mixing time as a function of specific power input for the BIOSTAT CultiBag STR (RT + SBI) is shown (**b**)

sources of mechanical stress. In the following sections, methods to determine mechanical stress for the UniVessel SU are discussed. The maximum power input is proportional to the mechanical stress (24).

4.4.1 Kolmogorov Length Scale

According to the theory that cells are damaged by eddies of comparable size, the size of the smallest turbulent eddies (λ), also referred to as the Kolmogorov microscale of turbulence, was determined assuming local isotopic turbulence according to (24). Smaller eddies do not possess the energy to harm the cells, and cells follow larger eddies convectively. The volume-averaged turbulence microscales predicted for the UniVessel SU are summarized in Fig. 6a, where the static fluid zone, the rotating zone of the stirrer, and the stirrer surface are shown.

The investigation of the volume-weighted averaged Kolmogorov length scale in the fluid domain and in the stirrer zone revealed values of between 50 and 400 μm. The minimum Kolmogorov length scales are determined directly at the stirrer sites and range between 32 and 9 μm (0.4 W/m^3 < P/V < 435 W/m^3). Furthermore, it was found that λ (24) correlates well with P/V as follows (26):

$$\lambda \propto (P/V)^{-m} \tag{26}$$

where m is 0.2 ± 0.01, a value that is near the theoretical value of 0.25 provided by (24). This agrees well with the literature and is almost identical to other single-use bioreactors [108]. Comparable values were also obtained for the BIOSTAT CultiBag STR product line, where the regions close to the stirrer and the rotating stirrer zone (as well as in the fluid zone, data not shown) were investigated (Fig. 6b). In addition, the Kolmogorov length scale increases if the scale increases, and thus the power input declines.

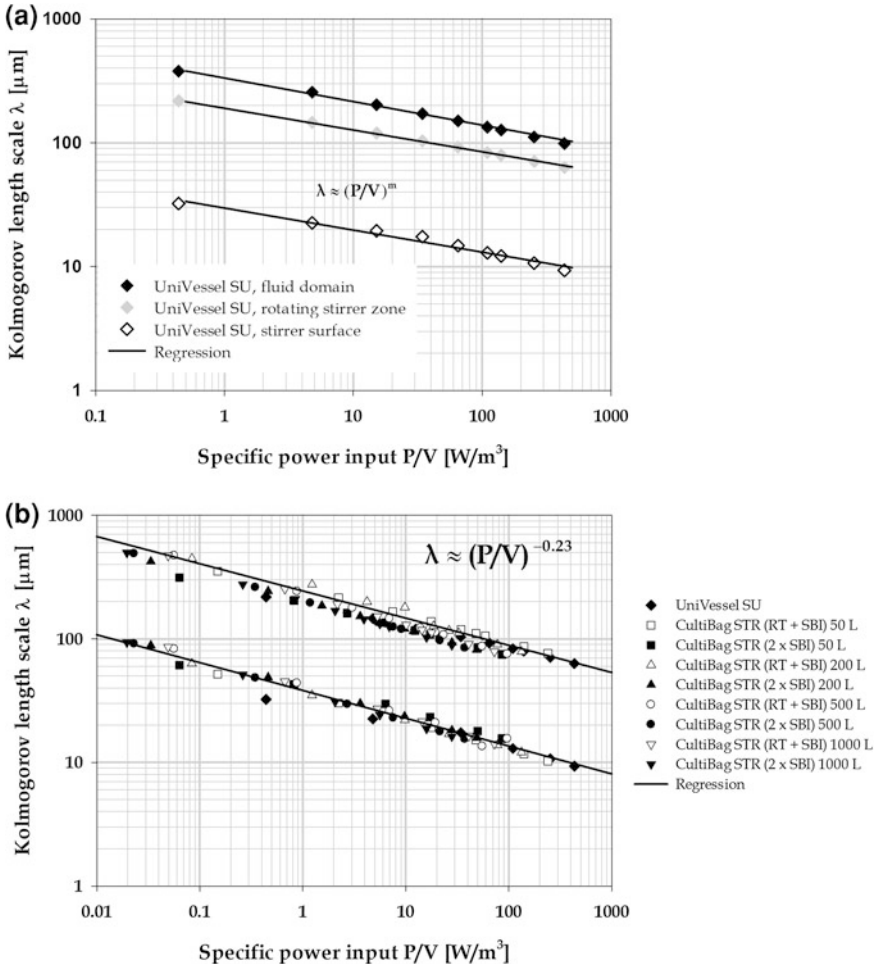

Fig. 6 Numerically predicted Kolmogorov length scale for the overall fluid domain, the rotating stirrer zone, and close to the stirrer surface as a function of specific power input in the UniVessel SU (**a**). The length scale close to the stirrer surface and in the rotating zone for all bioreactor sizes and configurations is shown in (**b**). The stirrer zone comprises the fluid that is directly in contact with the stirrer surface, whereas the rotating stirrer zone is made up of the stirrer movement volume. For all scales, the rotating stirrer volume is approximately 7 % of the total volume. The fluid domain represents the overall fluid without the rotating stirrer zones

When considering the size of CHO cells (10 µm $< d <$ 20 µm), no cellular damage is expected for either bioreactor type at meaningful power inputs, because the smallest eddies are significantly larger than the cells and, therefore, the cells will follow the eddies in a convective manner. In contrast, exceeding a *P/V* of 10 W/m^3 is expected to damage the cells in the region close to the stirrer,

inasmuch as the minimum Kolmogorov length scale is below 20 µm. However, this theory has not been proven thus far and describes a hypothesis (see Sect. 3.2).

4.4.2 Velocity Gradients

In addition to turbulence, cells are thought to be affected by velocity gradients, where shear and normal gradients (experimentally and numerically determined) can be distinguished [88, 108, 114]. Shear gradients were found to be dominant in stirred bioreactors [88, 114], and predominantly responsible for cell damage [181], therefore normal gradients have not been considered in the present study. The shear stress distribution, as given in (Fig. 7a), was obtained by discretizing the shear stress values into 250 bins and summing the volume elements where the shear stress occurred.

This volume-weighted distribution can be described by a logarithmic normal function, providing a maximum volume fraction of about 4.7 % in the UniVessel SU, irrespective of the specific power input (Fig. 7a). The local shear gradients (γ_{NT}) obtained for a maximum volume fraction (median value), increase proportionally to the third root of P/V from 2.4 up to 28 1/s [see (27); Fig. 7b]. The resultant exponent of 0.33 has already been published for the Single-Use Bioreactor (S.U.B.) and the BIOSTAT CultiBag STR 50 L (both stirrer configurations) in earlier experiments [108].

$$\gamma_{NT} \propto (P/V)^{1/3} \tag{27}$$

For the maximum P/V ($\approx$435 W/m^3), a maximum local shear gradient of $\sim$1,000 1/s was determined. According to Yim and Shamlou [182], the range of local shear gradients affecting the physiological state of the cells is between 500 and 5,000 1/s. Taking this into consideration, damage to the cells cultivated in the UniVessel SU at a maximum P/V cannot be excluded. Nevertheless, the numerically obtained mean and maximum shear gradient values are far beyond the critical values of 1–3 $\times$ 10^5 1/s which are known to damage the cells irreversibly [160].

4.5 Volumetric Mass Transfer Coefficient

The investigation of the volumetric mass transfer coefficient k_La was performed numerically using the Euler–Euler approach. As mentioned above, the k_La depends on, among other things, the (local) gas-holdup, the properties of the medium, and the size of the gas bubbles. These factors are primarily affected by the sparger and influenced by bubble coalescence and break-up processes. The experimental determination of the size of the gas bubbles was performed using photography [88] and sophisticated Shadowgraphy (Fig. 8a) as described in Ref. [207]. In the CFD models, a unique bubble size was assumed, although the prediction of bubble size

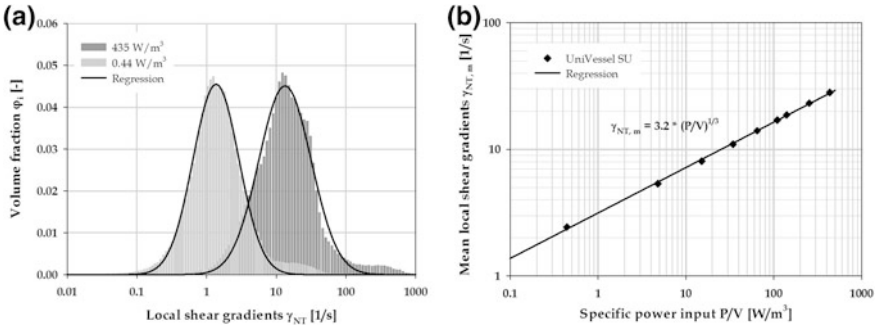

Fig. 7 Evaluation of the frequency distribution for the local shear gradients as a function of volume fraction in the UniVessel SU for a specific power input of 0.4 and 435 W/m^3 (**a**). Comparison of the mean local shear gradients as a function of specific power input in the UniVessel SU under transient ($0.4 < P/V < 34$ W/m^3) and turbulent ($34 < P/V < 435$ W/m^3) flow conditions (**b**)

distribution by population balance equation models has been shown to improve the accuracy of k_La determination. However, these models result in much higher computational demands. Depending on the cell line, high aeration rates or strong sparging can immediately damage the cells, however, this can be prevented if the aeration rate is below 0.1 vvm [183]. CHO cells, which represent the most often used production organism in the modern biopharmaceutical industry, have specific oxygen uptake rates on the order of 0.25–0.35 $\times$ 10^{-12} mol/cell/h [38, 184]. More detailed data for specific oxygen uptake rates of various cell lines is provided in Refs. [185, 186]. Due to the low oxygen requirements, k_La values on the order of 2–37 1/h are mostly sufficient to reach medium to high cell densities, as shown in Ref. [187].

In the UniVessel SU two-phase simulations were performed for P/Vs from 0.4 to 435 W/m^3, assuming an air bubble size of 1 mm. In order to analyze the k_La (18), superficial gas velocities of 2.8 $\times$ 10^{-4} and 5.7 $\times$ 10^{-4} m/s (corresponding to 0.1 and 0.2 vvm) were used (Fig. 8b). According to Zhu, the flow regimes resulting from these aeration rates and bubble diameters are not significantly altered [188]. The numerically determined k_La values (14 and 25) for the UniVessel SU at maximum working volume were plotted as a function of P/V (Fig. 8b). Depending on the aeration rate, k_La values ranging from 10–60 1/h (0.1 vvm) and 20–100 1/h (0.2 vvm) were found. Comparing the experimental results to the numerically obtained results, the latter deliver lower k_La values, which are, nevertheless, on the same order of magnitude [189]. However, these values are very high, meaning they are sufficient for aerobic microbial fermentations, requiring higher specific power inputs and aeration rates.

Increasing the P/V results in lower oxygen transfer resistance, due to the higher surface renewal rate of the bubbles [190] and, therefore, leads to higher mass transfer coefficient values of k_L and k_La, respectively. In both bioreactor types, the liquid mass transfer coefficient k_L ranges from 1.25–2.65 $\times$ 10^{-4} m/s (25). Based on these results, the maximum required k_La of 37 1/h mentioned above, has

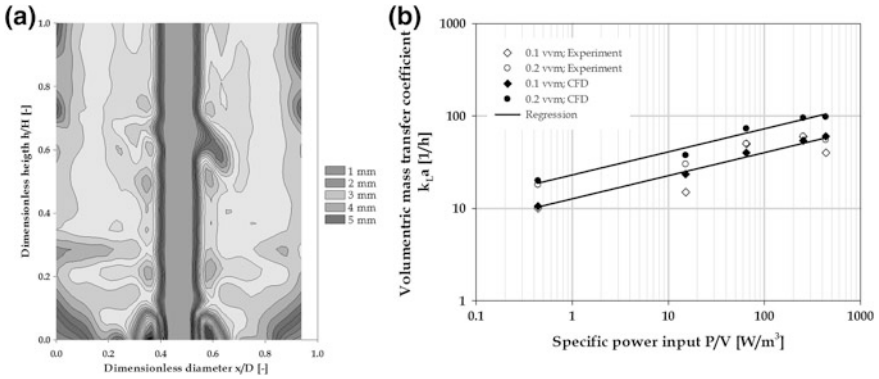

Fig. 8 Determination of the mean bubble diameter in the BIOSTAT CultiBag STR (RT + SBI) 50 L using Shadowgraphy (**a**). Experimentally and numerically-predicted volumetric oxygen mass transfer coefficients as a function of specific power input for the aeration rates of 0.1 and 0.2 vvm in the UniVessel SU (**b**)

already been achieved with a *P/V* of 90 W/m^3 at an aeration rate of 0.1 vvm, and an even lower *P/V* of 10 W/m^3 at 0.2 vvm. In the BIOSTAT CultiBag STR 50 L (both configurations; Fig. 8a), the mean bubble diameter was 5 mm and was measured using the Shadowgraphy technique at a P/V of 1.05 W/m^3 and an aeration rate of 0.02 vvm. In this case, a maximum k_La value of 35 1/h was determined at an aeration rate of 0.1 vvm [88] using the gassing-out method.

Using the correlation suggested by van't Riet in (18), which represents the k_La as a function of the specific power input and the superficial gas velocity, the coefficients C, x_1, and x_2 were found to be 0.4, 0.25, and 0.78, respectively (28). Here, the superficial gas velocity has a strong influence on the k_La value, whereas the specific power input is of only minor importance. This may be explained by the low dispersion capacity of the stirrer when operated at low agitation rates. These results were also found for other single-use bioreactors such as the Mobius CellReady 3 L bioreactor or a prototype of the UniVessel SU with a Rushton turbine and a segment blade impeller [88, 90].

$$k_La = 0.4 \cdot (P/V)^{0.25} \cdot u_G^{0.78} \tag{28}$$

5 Scale-up of Single-Use Bioreactors

A key element in the biopharmaceutical industry is the transfer of the cultivation process from lab to production scale (scale-up), while ensuring identical process characteristics [191]. The most often applied scale-up approach is based on geometric similarity (height to diameter ratio) and/or engineering parameters (e.g., u_{Tip}, P/V, θ_m, k_La, λ, γ_{NT}) of the bioreactor [171, 172, 183, 192].

In order to determine a bioreactor's engineering parameters, a fundamental engineering characterization is required (see Sect. 3), where the specific power input, mixing time, and volumetric mass transfer coefficient represent the most often used scale-up criteria [192, 193]. For microbial fermentations, the heat exchange surface has proven itself as a reliable scale-up factor [120] whereas in microcarrier-based stem cell cultivations the suspension criterion, where the microcarriers are homogeneously dispersed, has been successfully introduced [33, 194]. However, it is not possible to keep all parameters constant when scaling up [38, 192] and, therefore, a compromise must often be found under consideration of critical process parameters (e.g., oxygen transfer or specific power input), which have to be identified in advance [178].

The impeller speed, which is often used for scaling up in the pharmaceutical industry [88] is not a major parameter for scaling up [120, 172] and results in a decreasing of the specific power input. Based on a tip speed of 0.9 m/s, the specific power input is 118 W/m^3 in the UniVessel SU and decreases in the BIOSTAT CultiBag STR 1,000 L to 5 W/m^3. For bioreactors larger than benchtop scale, this leads to decreased mixing and mass transfer and results in unacceptable cell growth.

To prevent the formation of concentration gradients, mixing time represents a further criterion that can cause issues when scaling up. A relationship between the mixing time and bioreactor/stirrer type is provided in Eq. (11), based on the specific power input and the reactor as well as the stirrer geometry [120, 127, 195]. As shown in Fig. 9, the mixing times predicted for the different single-use bioreactors and sizes investigated in this study were well correlated by this single equation (with $R^2 = 0.97$). The determined proportional factor is 3.5, which is in the same range as the predicted value of 5.9 [195].

$$\theta_m = 3.5 \cdot (P/V)^{-1/3} \cdot (d_s/D)^{-1/3} \cdot (H/D)^{2.43} \cdot D^{2/3} \tag{29}$$

Especially at larger scales, inhomogeneous mixing contributes to the formation of pH and nutrient gradients as a result of local hydrodynamics [196], which may result in a reduction of cell growth and protein expression [127, 197, 198]. However, keeping mixing time constant when scaling up leads to a significant increase in the specific power input at larger scales [178, 199]. If the mixing time in the UniVessel SU is estimated to be 34 s (approximately 1 W/m^3), specific power inputs of 22 W/m^3 for the BIOSTAT CultiBag STR (2 × SBI) 500 L and 28 W/m^3 for the 1,000-L scale are required. According to (24), the Kolmogorov length scale in the stirrer zone and close to the stirrer decreases to 89 and 16 µm, respectively. In addition, an increase in the shear gradients can be observed due to the rising specific power input. When considering the working volume ($\gamma_{NT} \propto V^{-0.16}$) and the ratio of impeller diameter to vessel diameter ($\gamma_{NT} \propto d_s/D^{-2.7}$) (data generated by own studies, but not shown), correlation (30) results, showing a linear graph with a single proportional factor C for the UniVessel SU and the BIOSTAT CultiBag STR across the different scales (see Fig. 10). In the present study, C was found to be 0.05 (31). Considering the mixing time, as mentioned above, the mean local shear gradients are approximately 1.5 1/s (500 L,

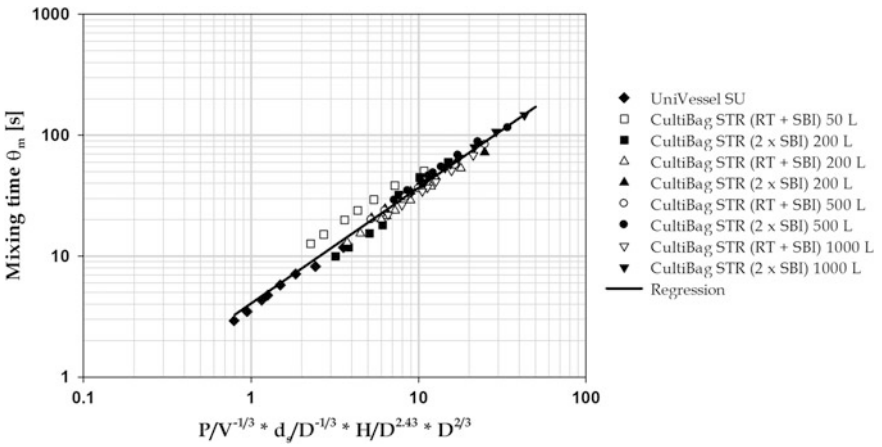

Fig. 9 Comparison of the CFD-predicted mixing times correlated by (11) for all bioreactor configurations investigated

21 W/m^3) and 1.4 1/s (1,000 L, 28 W/m^3), respectively. The maximum local shear gradients are below a value of 1,000 1/s (data not shown) and the Kolmogorov microscale is in a typical range for cell culture processes where no cell damage is expected (see Sect. 4.1, [160, 182]).

$$\gamma_{\mathrm{NT},m} = C \cdot (P/V)^{1/3} \cdot V^{-0.16} \cdot (d_s/D)^{-2.7} \tag{30}$$

$$\gamma_{\mathrm{NT},m} = 0.05 \cdot (P/V)^{1/3} \cdot V^{-0.16} \cdot (d_s/D)^{-2.7} \tag{31}$$

Specific power input has the largest influence on mass transfer and represents a successful compromise for scaling-up a bioreactor according to the Büche theorem [172]. Therefore, it is suggested that specific power input should be kept constant during scale-up, a technique that has been successfully applied in microbial fermentations and animal cell cultivations [38]. However, the scale-up with a constant specific power input results in an increase in mixing time, the Reynolds number and tip speed, whereas the stirrer speed, Froude number, and shear gradient, are decreased under turbulent flow conditions. In contrast, the eddy length scale remains constant according to (24).

In addition to the power input, oxygen mass transfer is a further scale-up criterion for aerobic processes. As already mentioned, animal cells have lower metabolic rates and oxygen demands than yeast and bacteria, but in high cell density processes, or in cases where aeration is limited by lack of mechanical stress tolerance, oxygen mass transfer can become a limiting factor [200]. If direct bubble aeration is applied, the risk of damaging the cells as a result of the bubbles bursting increases [160, 201–203, 147]. This risk also increases as the bubble diameter decreases [120].

The difficulty in scaling-up cell culture-based processes results from a lack of preservation of local flow structures as the reactor vessels are scaled-up [193]. It is

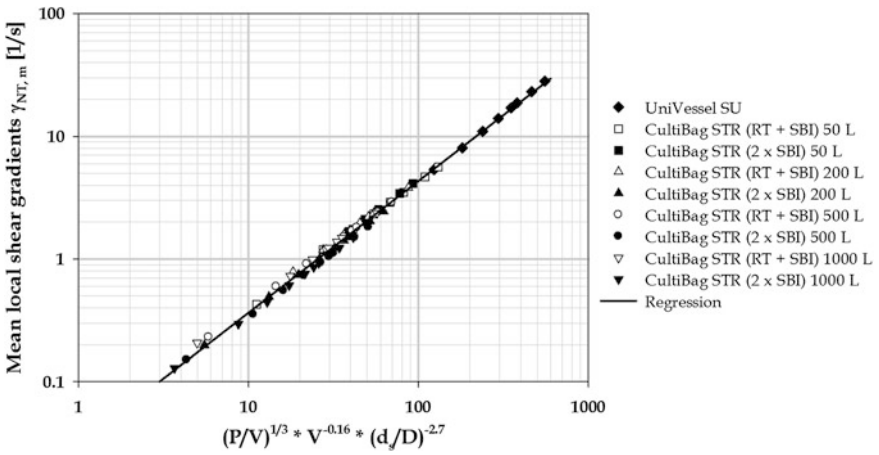

Fig. 10 Mean local shear gradients as a function of (30) for all single-use bioreactors investigated

well known that highly localized regions of high-energy dissipation exist and that local flow structures strongly depend on the vessel geometry and operating conditions. These local flow characteristics cannot be described adequately by global scale-up parameters. Therefore, engineering characterization is required, which consists of spatially resolved data obtained from experimental [193] and numerical methods. In order to turn the scaling-up of single-use bioreactors into a describable and understandable process, numerical techniques are increasingly being introduced in scale-up studies [204]. However, scaling up of bioreactors and processes remains a challenge and is "as much an art as a science" [205] and therefore, extensive know-how is presupposed [206].

6 Conclusions and Outlook

In this review, instrumented, commercially available single-use bioreactors from benchtop up to m^3 scale have been presented. Single-use bioreactors with entirely new working and aeration principles, such as wave-mixed, orbitally shaken, vibrating disk and rotatory oscillating systems, have established themselves during the past decade. However, the trend is moving more towards the development of bioreactors that are similar to conventional glass or stainless steel bioreactors and take mass transfer and power input from stirrers into account. This trend is independent of application and includes cell expansions, antibody and vaccine production, and manufacturing of secondary metabolites used in cosmetics.

The availability of bioengineering data speeds up the processes of selecting the most suitable single-use bioreactor type, defining process optimization parameters and scaling-up. In addition, it makes comparison with other single-use bioreactors

and their traditional counterparts possible, as shown for the UniVessel SU and the BIOSTAT CultiBag STR versions. In addition to established experimental methods, modern techniques such as CFD and PIV have become increasingly important. Their application has led to a reduction in experimental effort, time, and costs as well as ultimately contributing to more rapid product development and manufacturing.

Acknowledgments The results presented are part of a PhD thesis. The authors are grateful to Dipl.-Ing. Ute Husemann, Dr. Gerhard Greller, Dipl.-Ing. Jacqueline Herrman and Dr. Alexander Tappe, from Sartorius Stedim Biotech for providing geometric details for the bioreactors under investigation and experimental results for the BIOSTAT CultiBag STR, as well as for their participation in many helpful discussions.

References

1. Vanhamel S, Masy C (2011) Production of disposable bags: a manufacturer's report. In: Eibl R, Eibl D (eds) Single-use technology in biopharmaceutical manufacture. Wiley, Hoboken
2. Dechema (2011) Statuspapier des temporären Arbeitskreises: Single-Use-Technologie in der biopharmazeutischen Produktion.http://www.dechema.de/biotech_media/Downloads/StatPap_SingleUse_2011.pdf. Accessed 18 Nov 2012
3. Eibl D, Peuker T, Eibl R (2010) Single-use equipment in biopharmaceutical manufacture: a brief introduction. In: Eibl R, Eibl D (eds) Single-use technology in biopharmaceutical manufacture. Wiley, Hoboken
4. Brod H, Vester A, Kauling J (2012) Opportunities and limitations of disposable technologies in biopharmaceutical processes. Chem Ing Tech. doi:10.1002/cite.201100229
5. Maigetter RZ, Piombino T, Wood C et al (2010) Single-use (SU) systems. Encyclopedia of industrial biotechnology: bioprocess, bioseparation, and cell technology. doi:10.1002/9780470054581.eib116
6. Pietrzykowski M, Flanagan W, Pizzi V et al (2011) An environmental life cycle assessment comparing single-use and conventional process technology. BioPharm Int 24(S11):30–38
7. Merseburger T (2010) An introduction to the validation and qualification of disposables used in biomanufacture—a user's perspective. In: Eibl R, Eibl D (eds) Single-use technology in biopharmaceutical manufacture. Wiley, Hoboken
8. Bioplan Associates I (2012) 9th annual report and survey of biopharmaceutical manufacturing capacity and production: a study of biotherapeutic developers and contract manufacturing organizations. BioPlan Associates, Inc., Rockville
9. De Jesus M, Wurm FM (2011) Manufacturing recombinant proteins in kg-ton quantities using animal cells in bioreactors. Eur J Pharm Biopharm. doi:10.1016/j.ejpb.2011.01.005
10. Whitford WG (2012) Single-use Systems in animal cell-based bioproduction. In: Pathak Y, Benita S (eds) Animal cell-based bioproduction, in antibody-mediated drug delivery systems: concepts, technology, and applications. Wiley, Hoboken
11. Ratcliffe E, Glen KE, Workman VL et al (2012) A novel automated bioreactor for scalable process optimisation of haematopoietic stem cell culture. J Biotechnol. doi:10.1016/j.jbiotec.2012.06.025
12. Wen Y, Zang R, Zhang X et al (2012) A 24-microwell plate with improved mixing and scalable performance for high throughput cell cultures. Process Biochem. doi:10.1016/j.procbio.2011.12.023

13 Wenk P, Hemmerich J, Müller C et al (2012) Hochparallele Bioprozessentwicklung in geschüttelten Mikrobioreaktoren. Chem Ing Tech doi:10.1002/cite.201100206
14. Roberts I, Baila S, Rice RB et al (2012) Scale-up of human embryonic stem cell culture using a hollow fibre bioreactor. Biotechnol Lett. doi:10.1007/s10529-012-1033-1
15. Vaes B, Craeye D, Pinxteren J (2012) Quality control during manufacture of a stem cell therapeutic. BioProcess Int 10(S3):50–55
16. Furey J, Clark K, Card C (2011) Adoption of single-use sensors for bioprocess operations. BioProcess Int 9(S2):36–42
17. Lindner P, Endres C, Bluma A et al (2010) Disposable sensor systems. In: Eibl R, Eibl D (eds) Single-use systems in animal cell-based bioproduction. Wiley, Hoboken
18. Codner P, Cinat M (2005) Massive transfusion for trauma is appropriate. ITACCS. http://www.itaccs.com/traumacare/archive/05_03_Summer_2005/appropriate.pdf. Accessed 18 Nov 2012
19. Knazek RA, Gullino PM, Kohler PO et al (1972) Cell culture on artificial capillaries: an approach to tissue growth in vitro. Science 178(4056):65–66
20. Schwander E, Rasmusen H (2005) Scalable, controlled growth of adherent cells in a disposable, multilayer format. Genet Eng News 25(8):29
21. Eibl R, Kaiser S, Lombriser R et al (2010) Disposable bioreactors: the current state-of-the-art and recommended applications in biotechnology. Appl Microbiol Biotechnol. doi:10.1007/s00253-009-2422-9
22. Singh V (1999) Disposable bioreactor for cell culture using wave-induced agitation. Cytotechnology. doi:10.1023/a:1008025016272
23. Eibl D, Eibl R (2009) Bioreactors for mammalian cells: general overview. In: Eibl R, Eibl D, Pörtner R, Catapano G, Czermak P (eds) Cell and tissue reaction engineering. Springer, Berlin
24. Eibl R, Löffelholz C, Eibl D (2010) Single-use bioreactors: an overview. In: Eibl R, Eibl D (eds) Single-use systems in animal cell-based bioproduction. Wiley, Hoboken
25. Glazyrina J, Materne EM, Dreher T et al (2010) High cell density cultivation and recombinant protein production with *Escherichia coli* in a rocking-motion-type bioreactor. Microb Cell Fact. doi:10.1186/1475-2859-9-42
26. Lehmann N, Rischer H, Eibl D et al (2013) Wave-mixed and orbitally shaken single-use photobioreactors for diatom algae propagation. Chem Ing Tech. doi:10.1002/cite.201200137
27. Werner S, Eibl R, Lettenbauer C et al (2010) Innovative, non-stirred bioreactors in scales from milliliters up to 1000 liters for suspension cultures of cells using disposable bags and containers—a Swiss contribution. Chimia (Aarau) 64(11):819–823
28. Bögli NC, Ries C, Bauer I et al (2011) Bag-based rapid and safe seed-train expansion method for *Trichoplusia ni* suspension cells. BMC Proc. doi:10.1186/1753-6561-5-S8-P124
29. Eibl R, Werner S, Eibl D (2010) Bag bioreactor based on wave-induced motion: characteristics and applications. Adv Biochem Eng Biotechnol. doi:10.1007/10_2008_15
30. Rausch M, Pörtner R, Knäblein J (2013) Increase of the protein yield in high-five cells in a single-use perfusion bioreactor by a medium replacement. Chem Ing Tech. doi:10.1002/cite.201200121
31. Hami L, Chana H, Yuan V et al (2003) Comparison of a static process and a bioreactor-based process for the GMP manufacture of autologous ccellerated T-Cells for clinical trials. Bioprocess J 2(3):1–10
32. Hami LS, Green C, Leshinsky N et al (2004) GMP production and testing of Xcellerated T-Cells for the treatment of patients with CLL. Cytotherapy. doi:10.1080/14653240410005348
33. Hewitt CJ, Lee K, Nienow AW et al (2011) Expansion of human mesenchymal stem cells on microcarriers. Biotechnol Lett. doi:10.1007/s10529-011-0695-4
34. Kehoe D, Schnitzler A, Simler J et al (2012) Scale-up of human mesenchymal stem cells on microcarriers in suspension in a single-use bioreactor. BioPharm Int 25(3):28–38

35. Kauling J, Brod H, Jenne M et al (2012) Entwicklung der single-use BaySHAKE-Bioreaktortechnologie für die Kultivierung tierischer Zellen in Proceedings of the 14. In: Sperling R, Heiser M (eds) Köthener Rührer-Kolloquium 2011. Köthen/Anhalt, Hochschule Anhalt, Köthen
36. Klöckner W, Büchs J (2012) Advances in shaking technologies. Trends Biotechnol. doi:10.1016/j.tibtech.2012.03.001
37. Palomares LA, Ramirez OT (2010) Bioreactor scale-up. Encyclopedia of cell technology. doi:10.1002/0471250570.spi023
38. Xing Z, Kenty BM, Li ZJ et al (2009) Scale-up analysis for a CHO cell culture process in large-scale bioreactors. Biotechnol Bioeng. doi:10.1002/bit.22287
39. Eibl R, Brändli J, Eibl D (2012) Plant cell bioreactors. In: Doelle HW, Rokem S, Berovic M (eds) Encyclopedia of life support systems (EOLSS), Developed under the auspices of the UNESCO. Eolss Publishers, Oxford
40. Schultz JB, Giroux D (2011) 3-L to 2,500-L single-use bioreactors. BioProcess Int 9(7):120
41. Auton K, Bick J, Taylor I (2007) Application note: strategies for the culture of CHO-S cells. Genet Eng News 27(16). http://www.genengnews.com/gen-articles/application-note-strategies-for-the-culture-of-cho-s-cells/2208/. Accessed 18 Nov 2012
42. Auton KA (2006) Single use bioreactors: making the transmission. Innovations. http://www.iptonline.com/articles/public/page54555655859loresnonprint.pdf. Accessed 18 Nov 2012
43. Auton KA (2010) Single use bioreactors: expressing protein in mammalian cell suspension. In: Noll T (ed) Cells and culture. doi:10.1007/978-90-481-3419-9_12
44. Clincke MF, Molleryd C, Zhang Y et al (2011) Study of a recombinant CHO cell line producing a monoclonal antibody by ATF or TFF external filter perfusion in a WAVE bioreactor. BMC Proc. doi:10.1186/1753-6561-5-s8-p105
45. Haldankar R, Li D, Saremi Z et al (2006) Serum-free suspensin large-scale transient transfection of CHO cells in WAVE bioreactors. Mol Biotechnol. doi:10.1385/mb:34:2:191
46. Sadeghi A, Pauler L, Annerén C et al (2011) Large-scale bioreactor expansion of tumor-infiltrating lymphocytes. J Immunol Methods. doi:10.1016/j.jim.2010.11.007
47. Sellhorn G, Caldwell Z, Mineart C et al (2009) Improving the expression of recombinant soluble HIV envelope glycoproteins using pseudo-stable transient transfection. Vaccine. doi:10.1016/j.vaccine.2009.10.028
48. Tao Y, Yusuf-Makagiansar H, Shih J et al (2012) Novel cholesterol feeding strategy enables a high-density cultivation of cholesterol-dependent NS0 cells in linear low-density polyethylene-based disposable bioreactors. Biotechnol Lett. doi:10.1007/s10529-012-0915-6
49. Wang L, Hu H, Yang J et al (2012) High yield of human monoclonal antibody produced by stably transfected *Drosophila Schneider* 2 cells in perfusion culture using WAVE bioreactor. Mol Biotechnol. doi:10.1007/s12033-011-9484-5
50. Adams T, Noack U, Frick T et al (2011) Increasing efficiency in protein and cell production by combining single-use bioreactor technology and perfusion. BioPharm Int 24(5):4–11
51. Bentebibel S, Moyano E, Palazón J et al (2005) Effects of immobilization by entrapment in alginate and scale-up on paclitaxel and baccatin III production in cell suspension cultures of Taxus baccata. Biotechnol Bioeng. doi:10.1002/bit.20321
52. Eibl R, Eibl D (2006) Design and use of the Wave bioreactor for plant cell culture. In: Dutta Gupta S, Ibaraki Y (ed) Plant tissue culture engineering. Springer, Dordrecht
53. Hundt B, Best C, Schlawin N et al (2007) Establishment of a mink enteritis vaccine production process in stirred-tank reactor and Wave bioreactor microcarrier culture in 1–10L scale. Vaccine. doi:10.1016/j.vaccine.2007.02.061
54. Raven N, Schillberg S, Kirchhoff J et al (2010) Growth of BY-2 suspension cells and plantibody production in single-use bioreactors. In: Eibl R, Eibl D (eds) Single-use technology in biopharmaceutical manufacture. Wiley, Hoboken
55. Ries C, Wasem V, Karrer D et al (2012) A new approach for rapid development of *Spodoptera frugiperda*/BEVS-based processes. In: Jenkins N, Barron N, Alves P (ed)

Proceedings of the 21st annual meeting of the European Society for Animal Cell Technology (ESACT). doi:10.1007/978-94-007-0884-6_111
56. Thomassen YE, Van Der Welle JE, Van Eikenhorst G et al (2012) Transfer of an adherent Vero cell culture method between two different rocking motion type bioreactors with respect to cell growth and metabolic rates. Process Biochem. doi:10.1016/j.procbio.2011.11.006
57. Ullah M, Burns T, Bhalla A et al (2008) Disposable bioreactors for cells and microbes: productivities similar to those achieved with stirred tanks can be achieved with disposable bioreactors. BioPharm Int. http://www.biopharminternational.com/biopharm/Disposables/Disposable-Bioreactors-for-Cells-and-Microbes/ArticleStandard/Article/detail/566012. Accessed 19 Nov 2012
58. Weber W, Weber E, Geisse S et al (2002) Optimisation of protein expression and establishment of the Wave bioreactor for baculovirus/insect cell culture. Cytotechnology. doi:10.1023/a:1021102015070
59. Finesse-Wave, Finesse Solution, LLC, San Jose. http://www.finesse.com/pr-3-15-11. Accessed 09 July 2012
60. Brändli J, Müller M, Imseng N et al (2012) Antikörperproduktion in Pflanzenzellen: Prozessentwicklung und -übertragung vom 50 mL auf den 10L Massstab. Biospektrum 2:2–3
61. Müller M (2010) Realisierung eines zweistufigen Prozesses zur Plantibody-Produktion mit BY-2-Suspensionszellen im AppliFlex®-Bioreaktor. Bachelor thesis, Anhalt University of Applied Sciences, Köthen/Anhalt
62. Bout B (2012) High level protein production by CHOBC cells in CELL-tainer single-use bioreactors. Single-use technologie: part of bioprocessing & stem cells, London, England
63. Oosterhuis NMG, Van Der Heiden P (2010) Mass Transfer in the CELL-tainer® Disposable Bioreactor. In: Noll T (ed) Cells and Culture, vol 4. Springer, Netherlands, pp 371–373
64. Zijlstra GM, Oosterhuis N (2010) Cultivation of PER.C6 cells in the novel CELL-Tainer™ high-performance disposable bioreactor. In: Noll T (ed) Cells and culture. doi:10.1007/978-90-481-3419-9_140
65. XRS Bioreactor System, PALL Life Sciences, Port Washington, NY. http://www.pall.com/main/Biopharmaceuticals/Biopharm-Whats-Next.page?. Accessed 03 July 2012
66. Kauling J, Brod H, Jenne M et al (2013) Novel, rotary sscillated, scalable single-use bioreactor technology for the cultivation of animal cells. Chem Ing Tech. doi:10.1002/cite.201200155
67. Jia Q, Li H, Hui M et al (2008) A bioreactor system based on a novel oxygen transfer method. BioProcess Int 6(6):2–5
68. Li L, Shi M, Song Y et al (2009) A single-use, scalable perfusion bioreactor system. BioProcess Int 7(6):46–54
69. Sun B, Yu X, Kong W et al (2012) Production of influenza H1N1 vaccine from MDCK cells using a novel disposable packed-bed bioreactor. Appl Microbiol Biotechnol. doi:10.1007/s00253-012-4375-7
70. Anderlei T, Cesana C, De Jesus M et al (2009) Shaken bioreactors provide culture alternative. Genet Eng News 29(19). http://www.genengnews.com/gen-articles/shaken-bioreactors-provide-culture-alternative/3092/. Accessed 18 Nov 2012
71. Potera C (2011) Orbital shake bioreactors take on scale-up—excellgene's platform includes no moving parts, low shear force, and high gas transfer. Gen Eng News 31. http://www.genengnews.com/gen-articles/orbital-shake-b-bioreactors-b-take-on-scale-up/3643/. Accessed 18 Nov 2012
72. Tissot S (2011) OrbShake bioreactors for mammalian cell cultures: engineering and scale-up. Ph D thesis, EPFL, Lausanne
73. Tissot S, Farhat M, Hacker DL et al (2010) Determination of a scale-up factor from mixing time studies in orbitally shaken bioreactors. Biochem Eng J. doi:10.1016/j.bej.2010.08.005
74. Galliher P (2008) Achieving high-efficiency production with microbial technology in a single-use bioreactor platform. BioPharm Int 6(11):60–65

75. Galliher PM, Hodge G, Guertin P et al (2010) Single-use bioreactor platform for microbial fermentation. In: Eibl R, Eibl D (eds) Single-use technology in biopharmaceutical manufacture. Wiley, Hoboken
76. Luitjens A, Pralong A (2010) Going fully disposable—current possibilities: a case study from Crucell. In: Eibl R, Eibl D (eds) Single-use technology in biopharmaceutical manufacture. Wiley, Hoboken
77. Mardirosian D, Guertin P, Corwell J et al (2009) Scaling up a CHO-produced hormone–protein fusion product. BioPharm Int 7(S4):30–35
78. Minow B, Rogge P, Thompson K (2012) Implementing a fully disposable mAb manufacturing facility. BioProcess Int 10(6):48–57
79. Cierpa K, Eisberg C, Niss K et al (2013) hMSC production in disposable bioreactors with regards to GMP and PAT. Chem Ing Tech. doi:10.1002/cite.201200151
80. Kittredge A, Gowda S, Ring J et al (2011) Characterization and performance of the Mobius® CellReady 200 L bioreactor system: the next generation of single-use bioreactors. http://www.millipore.com/publications.nsf/a73664f9f981af8c852569b9005b4eee/eb6d1e15cb3aa21b852578b900479440/$FILE/PS32330000_EMD.pdf. Accessed 18 Nov 2012
81. Madrid LV, Lahille AP (2013) A comparison of single-use bioreactors for the pharmaceutical industry. Chem Ing Tech (in press)
82. Dreher T, Husemann U, Zahnow C et al (2012) High Cell Density Escherichia coli cultivation in different single-use bioreactor Systems. Chem Ing Tech. doi:10.1002/cite.201200122
83. Hähnel A, Pütz B, Iding K et al (2011) Evaluation of a disposable stirred tank bioreactor for cultivation of mammalian cells. BMC Proc 5(8):54
84. Hundt B, Mölle N, Stefaniak S et al (2011) Large pilot scale cultivation process study of adherent MDBK cells for porcine influenza: a virus propagation using a novel disposable stirred-tank bioreactor. BMC Proc 5(8):128
85. Noack U (2010) Scale-up. Göttingen, Germany
86. Noack U, Wilde DD, Verhoeye F et al (2011) Single-use stirred tank reactor BIOSTAT CultiBag STR: characterisation and applications. In: Eibl R, Eibl D (eds) Single-use technology in biopharmaceutical manufacture. Wiley, Hoboken
87. Hummel A (2012) Zellkulturbasierte Proteinexpressionen mit partiellem und vollständigem Medienaustausch. Bachelor thesis, Anhalt University of Applied Sciences, Köthen/Anhalt
88. Kaiser SC, Löffelholz C, Werner S et al (2011) CFD for characterizing standard and single-use stirred cell culture bioreactors. In: Minin IV, Minin OV (eds) Computational fluid dynamics technologies and applications. doi:10.5772/23496
89. Dekarski J (2010) Mobius® Cell Ready single-use 3-L bioreactor. BioProcess Int 8(7):124–126
90. Kaiser SC, Eibl R, Eibl D (2011) Engineering characteristics of a single-use stirred bioreactor at bench-scale: the Mobius CellReady 3L bioreactor as a case study. Eng Life Sci. doi:10.1002/elsc.201000171
91. Gossain V, Mirro R (2012) Linear scale-up of cell cultures. BioProcess Int 8(11):56–62
92. George M, Farooq M, Dang T et al (2010) Production of cell culture (MDCK) derived live attenuated influenza vaccine (LAIV) in a fully disposable platform process. Biotechnol Bioeng. doi:10.1002/bit.22753
93. Goedde A, Reiser S, Russ K et al (2009) Characterisation of two single-use bioreactors for mammalian cell culture processes. http://rentschler.de/en/information/lectures-and-posters/page.pdf. Accessed 18 Nov 2012
94. Valasek C, Coke J, Hensel F et al (2011) Production and purificationof a PER.C6-expressed IgM antibody therapeutic. BioPharm Int 9(11):28–37
95. Calvosa E (2009) Large scale disposable bioreactor for vaccines manufacturing—applications to anchorage dependent cell line. In: IBC's 6th international single use applications for biopharmaceutical manufacturing, San-Diego

96. Rodriguez R, Castillo J, Giraud S (2010) Demonstrated performance of a disposable bioreactor with an anchorage-dependent cell line. BioProcess Int 8(8):74–78
97. Lee B, Fang D, Croughan M et al (2011) Characterization of novel pneumatic mixing for single-use bioreactor application. BMC Proc. doi:10.1186/1753-6561-5-s8-o12
98. Drugmand JC, Dubois S, Dohogne Y et al (2010) Viral entities production at manufacturing scale using the Integrity™ iCELLis™ disposable fixed-bed reactor. http://www.atmi.com/ls-assets/pdfs/bioreactors/icellis/Integrity_iCELLis_Poster_ESACT_Digital_A4.pdf. Accessed 18 Nov 2012
99. Drugmand JC, Havelange N, Collignon F et al (2012) 4 g/L.day: monoclonal antibody volumetric productivity in the iCELLisTM disposable fixed-bed bioreactor. In: Jenkins N, Barron N, Alves P (eds) Proceedings of the 21st annual meeting of the Europe and society for animal cell technology (ESACT), Dublin, Ireland, vol 5. Springer, Netherlands, pp 375–378, June 7–10 2009
100. Hambor JE (2012) Bioreactor design and bioprocess controls for industrialized cell processing. BioProcess Int 10(6):22–33
101. Prieels JP, Stragier P, Lesage F et al (2012) Mastering industrialization of cell therapy products. BioProcess Int 10(S3):12–15
102. Eibl R, Eibl D (2009) Application of disposable bag bioreactors in tissue engineering and for the production of therapeutic agents. In: Kasper C, Griensven M, Pörtner R (eds) Bioreactor systems for tissue engineering. Springer, Berlin
103. Agrawal V, Bal M (2012) Strategies for rapid production of therapeutic proteins in mammalian cells. BioPharm Int 10(4):32–48
104. Schirmer EB, Kuczewski M, Golden K et al (2010) Primary clarification of very high-density cell culture harvests by enhanced cell settling. BioProcess Int 8(1):32–39
105. Schmid D, Schürch C, Blum P et al (2008) Plant stem cell extract for longevity of skin and hair. SöFW 5:29–35
106. Sederma http://www.sederma.fr/home.aspx?s=111&r=127&p=3346. Accessed 16 Nov 2012
107. Hitchcook T (2009) Production of recombinant protein whole-cell vaccines with disposable manufacturing systems. BioProcess Int 5:36–46
108. Löffelholz C, Kaiser SC, Werner S et al (2012) Beitrag zur Charakterisierung und zum Einsatz des 50 L Single-Use Bioreactor (S.U.B.) in der biopharmazeutischen Industrie. In: Sperling R, Heiser M (eds) Proceedings of the 14. Köthener Rührer-Kolloquium 2011. Köthen/Anhalt, Hochschule Anhalt, Köthen
109. Löffelholz C, Kaiser SC, Werner S et al (2011) CFD as a tool to characterize single-use bioreactors. In: Eibl R, Eibl D (eds) Single-use technology in biopharmaceutical manufacture. Wiley, Hoboken
110. Liepe F, Sperling R, Jembere S (1998) Rührwerke—Theoretische Grundlagen, Auslegung und Bewertung, Eigenverlag FH Anhalt Köthen, Germany
111. Büchs J, Maier U, Milbradt C et al (2000) Power consumption in shaking flasks on rotary shaking machines: II. Nondimensional description of specific power consumption and flow regimes in unbaffled flasks at elevated liquid viscosity. Biotechnol Bioeng. doi:10.1002/(SICI)1097-0290(20000620)68:6<594:AID-BIT2>3.0.CO;2-U
112. Tan R-K, Eberhard W, Büchs J (2011) Measurement and characterization of mixing time in shake flasks. Chem Eng Sci. doi:10.1016/j.ces.2010.11.001
113. Stoots CM, Calabrese RV (1995) Mean velocity field relative to a Rushton turbine blade. AIChE J. doi:10.1002/aic.690410102
114. Wollny S (2010) Experimentelle und numerische Untersuchungen zur Partikel-beanspruchung in gerührten (Bio-)Reaktoren. Dissertation, Technische Universität, Berlin
115. Kaiser SC, Löffelholz C, Werner S et al (2011) CFD for characterizing standard and single-use stirred cell culture bioreactors. In: Minin IV, Minin OV (eds) Computational fluid dynamics technologies and applications. doi:10.5772/23496

116. Löffelholz C, Husemann U, Greller G et al (2013) Bioengineering parameters for single-use bioreactors: an overview and evaluation of suitable methods. Chem Ing Tech. doi:10.1002/cite.201200125
117. Büchs J, Maier U, Milbradt C et al (2000) Power consumption in shaking flasks on rotary shaking machines: I. Power consumption measurement in unbaffled flasks at low liquid viscosity. Biotechnol Bioeng. doi:10.1002/(sici)1097-0290(20000620)68:6<589:aid-bit1>3.0.co;2-j
118. Kato Y, Peter CP, Akgün A et al (2004) Power consumption and heat transfer resistance in large rotary shaking vessels. Biochem Eng J. doi:10.1016/j.bej.2004.04.011
119. Raval K, Kato Y, Buechs J (2007) Comparison of torque method and temperature method for determination of power consumption in disposable shaken bioreactors. Biochem Eng J. doi:10.1016/j.bej.2006.12.017
120. Nienow AW (2006) Reactor engineering in large scale animal cell culture. Cytotechnology. doi:10.1023/A:1008008021481
121. Chisti MY (1989) Airlift bioreactors. Elsevier, London
122. Meyer J (2011) Untersuchungen zum Einfluss von Blasenbegasung auf Stofftransport, Partikelbeanspruchung und Mischverhalten im oszillierenden BaySHAKE Einwegbioreaktorsystem. Diploma thesis, Hochschule für Technik und Wirtschaft, Berlin
123. Poles-Lahille A, Richard C, Fisch S et al (2011) Disposable bioreactors: from process development to production. BMC Proc 5(S8):2
124. Raval K (2008) Characterization and application of large disposable shaking bioreactors. Rheinisch-Westfälische Technische Hochschule Aachen, Germany
125. Ries C (2008) Untersuchungen zum Einsatz von Einwegbioreaktoren für die auf Insektenzellen basierte Produktion von internen und externen Proteinen. Diploma thesis, Zurich University of Applied Sciences (ZHAW), Wädenswil
126. Sadeli AR (2011) Detection of circulating tumor cells in peripheral blood and mixing time quantification in Millipore disposable bioreactors. Master thesis, Ohio State University, Columbus
127. Nienow AW (2010) Impeller selection for animal cell culture. Encyclopedia of industrial biotechnology: bioprocess, bioseparation, and cell technology. doi:10.1002/9780470054581.eib636
128. Zhang H, Williams-Dalson W, Keshavarz-Moore E et al (2005) Computational-fluid-dynamics (CFD) analysis of mixing and gas-liquid mass transfer in shake flasks. Biotechnol Appl Biochem. doi:10.1042/ba20040082
129. Zhang X, Bürki C-A, Stettler M et al (2009) Efficient oxygen transfer by surface aeration in shaken cylindrical containers for mammalian cell cultivation at volumetric scales up to 1000 L. Biochem Eng J. doi:10.1016/j.bej.2009.02.003
130. Doig SD, Pickering SCR, Lye GJ et al (2005) Modelling surface aeration rates in shaken microtitre plates using dimensionless groups. Chem Eng Sci. doi:10.1016/j.ces.2004.12.025
131. Hermann R, Lehmann M, Büchs J (2003) Characterization of gas–liquid mass transfer phenomena in microtiter plates. Biotechnol Bioeng. doi:10.1002/bit.10456
132. Zhang Q, Yong Y, Mao Z-S et al (2009) Experimental determination and numerical simulation of mixing time in a gas–liquid stirred tank. Chem Eng Sci. doi:10.1016/j.ces.2009.03.030
133. Garcia-Ochoa F, Gomez E (2009) Bioreactor scale-up and oxygen transfer rate in microbial processes: an overview. Biotechnol Adv. doi:10.1016/j.biotechadv.2008.10.006
134. Kittredge Wood A, Gowda S, Dinn L et al (2011) Use of small-scale, single-use bioreactors for streamlining upstream process development. Bioprocess J 10(1):34–39
135. Linek V, Vacek V, Benes P (1987) A critical review and experimental verification of the correct use of the dynamic method for the determination of oxygen transfer in aerated agitated vessels to water, electrolyte solutions and viscous liquids. Biochem Eng J. doi:10.1016/0300-9467(87)85003-7
136. Fietz F (2012) Messungen des Sauerstofftransfers und -verbrauchs von Zellkulturen in Einwegbioreaktoren. Master thesis, Anhalt University of Applied Sciences, Köthen/Anhalt

137. Mikola M, Seto J, Amanullah A (2007) Evaluation of a novel Wave bioreactor cellbag for aerobic yeast cultivation. Bioprocess Biosyst Eng. doi:10.1007/s00449-007-0119-y
138. Hermann R, Walther N, Maier U et al (2001) Optical method for the determination of the oxygen-transfer capacity of small bioreactors based on sulfite oxidation. Biotechnol Bioeng. doi:10.1002/bit.1126
139. Linek V, Sinkule J, Bener P (1991) Critical assessment of gassing-in methods for measuring k_La in fermentors. Biotechnol Bioeng. doi:10.1002/bit.260380402
140. Reith T, Beek WJ (1973) The oxidation of aqueous sodium sulphite solutions. Chem Eng Sci. doi:10.1016/0009-2509(73)80084-3
141. Backoff T, Malig J, Werner S et al (2012) Where does the oxygen go? k_La measurement in bioreactors. G.I.T. Lab J 9(10):21–22
142. Maier U, Büchs J (2001) Characterisation of the gas–liquid mass transfer in shaking bioreactors. Biochem Eng J. doi:10.1016/s1369-703x(00)00107-8
143. Funke M (2010) Microfluidic bioprocess control in baffled microtiter plates. Ph D thesis, RWTH Aachen, Germany
144. Maier U, Losen M, Büchs J (2004) Advances in understanding and modeling the gas–liquid mass transfer in shake flasks. Biochem Eng J. doi:10.1016/s1369-703x(03)00174-8
145. Rodrigues ME, Costa AR, Henriques M et al (2012) Wave characterization for mammalian cell culture: residence time distribution. N Biotechnol. doi:10.1016/j.nbt.2011.10.006
146. Hummel A (2012) Verfahrenstechnische Charakterisierung eines neuartigen single-use Bioreaktors. Semester thesis, Anhalt University of Applied Sciences, Köthen/Anhalt, Germany.
147. Galliher PM (2007) Review of single use technologies in biomanufacturing. http://www.wpi.edu/Images/CMS/BEI/parrishgalliher.pdf. Accessed 18 Nov 2012
148. Pneumatic Bioreactor System, PBSBiotech, Inc., Camarillo, CA. http://pbsbiotech.com/products-technology/. Accessed 27 June 2012
149. Höfken M, Schäfer M, Durst F (1996) Detaillierte Untersuchung des Strömungsfeldes innerhalb eines Sechs-Blatt-Scheibenrührers. Chem Ing Tech. doi:10.1002/cite.330680707
150. Venkat RV, Stock LR, Chalmers JJ (1996) Study of hydrodynamics in microcarrier culture spinner vessels: a particle tracking velocimetry approach. Biotechnol Bioeng. doi:10.1002/(sici)1097-0290(19960220)49:4<456:aid-bit13>3.0.co;2-8
151. Öncül AA, Lalmbach A, Genzel Y et al (2010) Characterisation of flow conditions in 2 L and 20 L wave bioreactor using computational fluid dynamics. Biotechnol Prog. doi:10.1002/btpr.312
152. Hutmacher DW, Singh H (2008) Computational fluid dynamics for improved bioreactor design and 3D culture. Trends Biotechnol. doi:10.1016/j.tibtech.2007.11.012
153. Batchelor GK (2000) An introduction to fluid dynamics. Cambridge University Press, Cambridge
154. Blazek J (2001) Computational fluid dynamics: principles and applications. Elsevier, Amsterdam
155. Lomax H, Pulliam T, Zingg D (2001) Fundamentals of computational fluid dynamics. Springer, Berlin
156. Paschedag AR (2004) CFD in der Verfahrenstechnik—Allgemeine Grundlagen und mehrphasige Anwendungen. Wiley-VCH, Weinheim
157. Wesseling P (2001) Principles of computational fluid dynamics. Springer, Berlin
158. Löffelholz C, Werner S, Ay P et al (2010) Untersuchungen zum Strömungsverhalten des Einweg-Vibromix-Bioreaktors. In: Egbers C, Ruck B, Leder A, Dopheide D (eds) Proceedings of the 18. GALA-Fachtagung “Lasermethoden in der Strömungsmesstechnik”, Cottbus, Germany
159. Zhang H, Lamping SR, Pickering SCR et al (2008) Engineering characterisation of a single well from 24-well and 96-well microtitre plates. Biochem Eng J. doi:10.1016/j.bej.2007.12.005
160. Chisti Y (2001) Hydrodynamic damage to animal cells. Crit Rev Biotechnol. doi:10.1080/20013891081692

161. Croughan MS, Sayre ES, Wang DIC (1989) Viscous reduction of turbulent damage in animal cell culture. Biotechnol Bioeng. doi:10.1002/bit.260330710
162. Kunas KT, Papoutsakis ET (2009) Damage mechanisms of suspended animal cells in agitated bioreactors with and without bubble entrainment. Biotechnol Bioeng 102(4):977–987. doi:10.1002/bit.22263
163. Dhanasekharan KM, Sanyal J, Jain A et al (2005) A generalized approach to model oxygen transfer in bioreactors using population balances and computational fluid dynamics. Chem Eng Sci. doi:10.1016/j.ces.2004.07.118
164. Kerdouss F, Bannari A, Proulx P et al (2008) Two-phase mass transfer coefficient prediction in stirred vessel with a CFD model. Comput Chem Eng. doi:10.1016/j.compchemeng.2007.10.010
165. Bujalski JM, Yang W, Nikolov J et al (2006) Measurement and CFD simulation of single-phase flow in solvent extraction pulsed column. Chem Eng Sci. doi:10.1016/j.ces.2005.10.057
166. Nakiboğlu G, Gorlé C, Horváth I et al (2009) Stack gas dispersion measurements with large scale-PIV, aspiration probes and light scattering techniques and comparison with CFD. Atmos Environ. doi:10.1016/j.atmosenv.2009.03.047
167. Torré J-P, Fletcher DF, Lasuye T et al (2007) Single and multiphase CFD approaches for modelling partially baffled stirred vessels: comparison of experimental data with numerical predictions. Chem Eng Sci. doi:10.1016/j.ces.2007.06.044
168. Alcamo R, Micale G, Grisafi F et al (2005) Large-eddy simulation of turbulent flow in an unbaffled stirred tank driven by a Rushton turbine. Chem Eng Sci. doi:10.1016/j.ces.2004.11.017
169. Montante G, Lee KC, Brucato A et al (2001) Numerical simulations of the dependency of flow pattern on impeller clearance in stirred vessels. Chem Eng Sci. doi:10.1016/s0009-2509(01)00089-6
170. Yianneskis M, Popiolek Z, Whitelaw JH (1987) An experimental study of the steady and unsteady flow characteristics of stirred reactors. J Fluid Mech. doi:10.1017/S002211208700051X
171. Zlokarnik M (2006) Scale-up in chemical engineering. Wiley-VCH, Weinheim
172. Kraume M (2003) Mischen und Rühren: Grundlagen und moderne Verfahren. Wiley-VCH, Weinheim
173. Zlokarnik M (1999) Rührtechnik—Theorie und Praxis. Springer, Berlin
174. Henzler HJ (2000) Particle stress in bioreactors. Adv Biochem Eng Biotechnol. doi:10.1007/3-540-47865-5_2
175. Garcia-Ochoa F, Gomez E, Santos V et al (2010) Oxygen uptake rate in microbial processes: an overview. Biochem Eng J. doi:10.1016/j.bej.2010.01.011
176. Jahoda M, Moštěk M, Kukuková A et al (2007) CFD modelling of liquid homogenization in stirred tanks with one and two impellers using large eddy simulation. Chem Eng Res Des. doi:10.1205/cherd06183
177. Min J, Gao Z (2006) Large eddy simulations of mixing time in a stirred tank. Chin J Chem Eng 14(1):1–7. doi:10.1016/s1004-9541(06)60030-x
178. Storhas W (1994) Bioreaktoren und periphere Einrichtungen ein Leitfaden für die Hochschulausbildung, für Hersteller und Anwender. Vieweg, Braunschweig
179. Jaworski Z, Nienow AW, Koutsakos E et al (1991) An LDA study of turbulent flow in a baffled vessel agitated by a pitched blade turbine. Elsevier, Amsterdam, PAYS-BAS
180. Ranade VV, Joshi JB (1989) Flow generated by pitched blade turbines I: measurements using laser Doppler anemometer. Chem Eng Commun. doi:10.1080/00986448908940539
181. Langer G, Deppe A (2000) Zum Verständnis der hydrodynamischen Beanspruchung von Partikeln in turbulenten Rührerströmungen. Chem Ing Tech. doi:10.1002/1522-2640(200001)72:1/2<31:AID-CITE31>3.0.CO;2-O
182. Yim S, Shamlou P (2000) The engineering effects of fluids flow on freely suspended biological macro-materials and macromolecules. In: Schügerl K, Kretzmer G, Henzler H,

Kieran P, Macloughlin P, Malone D, Schumann W, Shamlou P, Yim S (eds) Influence of stress on cell growth and product formation. Springer, Berlin
183. Czermak P, Pörtner R, Brix A (2009) Special engineering aspects. In: Eibl R, Eibl D, Pörtner R, Catapano G, Czermak P (eds) Cell and tissue reaction engineering. Springer, Berlin
184. Ducommun P, Ruffieux P-A, Furter M-P et al (2000) A new method for on-line measurement of the volumetric oxygen uptake rate in membrane aerated animal cell cultures. J Biotechnol. doi:10.1016/s0168-1656(99)00237-0
185. Godoy-Silva R, Berdugo C, Chalmers JJ (2010) Aeration, mixing, and hydrodynamics, animal cell bioreactors. Encyclopedia of industrial biotechnology: bioprocess, bioseparation, and cell technology. doi:10.1002/9780470054581.eib010
186. Ruffieux P-A, Von Stockar U, Marison IW (1998) Measurement of volumetric (OUR) and determination of specific (qO2) oxygen uptake rates in animal cell cultures. J Biotechnol. doi:10.1016/s0168-1656(98)00046-7
187. Zijlstra G, Noack U, Weisshaar S et al (2011) High cell density XD cultivation of CHO cells in BIOSTAT CultibBag STR 50 L single-use bioreactor with novel microsparger and single-use exhaust cooler. http://microsite.sartorius.com/fileadmin/Image_Archive/microsite/biostat_cultibag_str/pdf/11-06-21/DSM_ESCAT_Sartorius.pdf. Acessed 04.03.2013
188. Zhu H, Nienow AW, Bujalski W et al (2009) Mixing studies in a model aerated bioreactor equipped with an up- or a down-pumping elephant ear agitator: power, hold-up and aerated flow field measurements. Chem Eng Res Des. doi:10.1016/j.cherd.2008.08.013
189. Löffelholz C, Werner S, Kaiser SC et al (2012) Comparative studies of single-use stirred bioreactors by means of traditional methods, CFD and cultivation experiments Frankfurt, Germany
190. Gimbun J, Nagy Z, Rielly C (2008) CFD and population balance modelling of gas-liquid flow via QMOM with moment correction function. In: Proceedings of the sixth international symposium on mixing in industrial process industries—ISMIP VI, Niagara on the Lake, Niagara Falls, Ontario, Canada
191. Vorlop J, Lehmann J (1988) Scale-up of bioreactors for fermentation of mammalian cell cultures, with special reference to oxygen supply and microcarrier mixing. Chem Eng Technol. doi:10.1002/ceat.270110123
192. Varley J, Birch J (1999) Reactor design for large scale suspension animal cell culture. Cytotechnology. doi:10.1023/a:1008008021481
193. Venkat RV, Chalmers JJ (1996) Characterization of agitation environments in 250 ml spinner vessel, 3 L, and 20 L reactor vessels used for animal cell microcarrier culture. Cytotechnology. doi:10.1007/bf00353928
194. Kaiser SC, Jossen V, Schirmaier C et al (2013) Fluid Flow and Cell Proliferation of Mesenchymal Adipose-Derived Stem Cells in Small-Scale, Stirred, Single-Use Bioreactors. Chem Ing Tech. doi:10.1002/cite.201200180
195. Nienow AW (1997) On impeller circulation and mixing effectiveness in the turbulent flow regime. Chem Eng Sci. doi:10.1016/s0009-2509(97)00072-9
196. Langheinrich C, Nienow AW (1999) Control of pH in large-scale, free suspension animal cell bioreactors: alkali addition and pH excursions. Biotechnol Bioeng. doi:10.1002/(sici)1097-0290(1999)66:3<171:aid-bit5>3.0.co;2-t
197. Osman JJ, Birch J, Varley J (2001) The response of GS-NS0 myeloma cells to pH shifts and pH perturbations. Biotechnol Bioeng. doi:10.1002/bit.1165
198. Osman JJ, Birch J, Varley J (2002) The response of GS-NS0 myeloma cells to single and multiple pH perturbations. Biotechnol Bioeng. doi:10.1002/bit.10198
199. Junker BH (2004) Scale-up methodologies for *Escherichia coli* and yeast fermentation processes. J Biosci Bioeng. doi:10.1016/s1389-1723(04)70218-2
200. Ozturk SS (1996) Engineering challenges in high density cell culture systems. Cytotechnology. doi:10.1007/bf00353919
201. Handa A, Emery AN, Spier RE (1987) On the evaluation of gas-liquid interfacial effects on hybridoma viability in bubble column bioreactors. Dev Biol Stand 66:241–253

202. Jöbses I, Martens D, Tramper J (1991) Lethal events during gas sparging in animal cell culture. Biotechnol Bioeng. doi:10.1002/bit.260370510
203. Oh SKW, Nienow AW, Al-Rubeai M et al (1992) Further studies of the culture of mouse hybridomas in an agitated bioreactor with and without continuous sparging. J Biotechnol. doi:10.1016/0168-1656(92)90144-x
204. Letellier B, Xuereb C, Swaels P et al (2002) Scale-up in laminar and transient regimes of a multi-stage stirrer, a CFD approach. Chem Eng Sci. doi:10.1016/s0009-2509(02)00371-8
205. Ma N, Chalmers JJ, Mollet M (2006) Aeration, mixing and hydrodynamics in bioreactors. In: Ozturk SS, Hu W-S (eds) Cell culture technology for pharmaceutical and cell-based therapies. CRC Press, New York
206. Catapano G, Czermak P, Eibl R et al (2009) Bioreactor design and scale-up. In: Eibl R, Eibl D, Pörtner R, Catapano G, Czermak P (eds) Cell and tissue reaction engineering. Springer, Berlin
207. Jossen V (2012) Bestimmung der Blasengrössenverteilung in einem modernen Zellkulturbioreaktor mittels PIV/Shadowgraphy. Semester thesis, Zurich University of Applied Sciences, Wädenswil